A regulatory T cell Notch4-GDF15 axis licenses tissue inflammation in asthma

Hani Harb[1,2], **Emmanuel Stephen-Victor**[1,2], **Elena Crestani**[1,2], **Mehdi Benamar**[1,2], **Amir Massoud**[1,2], **Ye Cui**[1,2], **Louis-Marie Charbonnier**[1,2], **Sena Arbag**[1], **Safa Baris**[3], **Amparito Cunnigham**[1], **Juan Manuel Leyva-Castillo**[1,2], **Raif S. Geha**[1,2], **Amirhosein J. Mousavi**[4], **Boris Guennewig**[5], **Klaus Schmitz-Abe**[1,6], **Constantinos Sioutas**[4], **Wanda Phipatanakul**[1,2], **Talal A. Chatila**[1,2]

[1]Division of Immunology, Boston Children's Hospital, Boston, MA, 02115 USA.

[2]Department of Pediatrics, Harvard Medical School, Boston, MA, 02115 USA;

[3]Division of Pediatric Allergy/Immunology, Marmara University Faculty of Medicine, Istanbul, Turkey;

[4]Department of Civil and Environmental Engineering, University of Southern California, CA, USA;

[5]Sydney Medical School, Brain and Mind Centre, The University of Sydney, Camperdown, Sydney, NSW, Australia;

[6]Division of Newborn Medicine, Boston Children's Hospital, Harvard Medical School, MA, USA;

Abstract

Elucidating the mechanisms that sustain asthmatic inflammation is critical for precision therapies. We found that IL-6 and STAT3 transcription factor-dependent upregulation of Notch4 receptor on lung tissue regulatory T (T_{reg}) cells is necessary for allergens and particulate matter pollutants to promote airway inflammation. Notch4 subverted T_{reg} cells into T_H2 and T_H17 effector T (T_{eff}) cells by Wnt and Hippo pathway-dependent mechanisms. Wnt activation induced growth and differentiation factor 15 (GDF15) expression in T_{reg} cells, which activated group 2 innate

lymphoid cells (ILC2) to provide a feed-forward mechanism for aggravated inflammation. Notch4, Wnt and Hippo were upregulated on circulating T_{reg} cells of asthmatics as a function of disease severity, in association with reduced T_{reg} cell-mediated suppression. Our studies thus identify Notch4-mediated immune tolerance subversion as a fundamental mechanism that licenses tissue inflammation in asthma.

A hallmark of asthma is a chronic inflammatory process that is associated with airway hyper-responsiveness and tissue remodeling[1, 2]. The persistence of asthmatic inflammation in the face of countervailing immunoregulatory mechanisms that normally limit tissue damage suggests that the latter may become compromised[3]. In agreement with this premise, subversion of allergen-specific Foxp3^{+} T regulatory (T_{reg}) cells, leading to the loss of their immune regulatory activity and their conversion into T helper type 2 (T_H2) and type 17 (T_H17) T effector (T_{eff})-like cells, has emerged as a key pathogenic mechanism[3, 4, 5, 6]. Elucidating the molecular mechanisms of T_{reg} cell subversion in asthma and means of restoring their function would offer novel approaches to therapy.

Relevant to immune tolerance breakdown in allergic airway inflammation are recent studies on mechanisms by which air polluting ambient particulate matter (PM), and especially ultrafine particles (UFP), upregulate allergic airway inflammation[7, 8]. These particles are taken up by alveolar macrophages, where they activate the aryl hydrocarbon receptor to induce the expression of the Notch ligand Jagged1 (Jag1). In turn, Jag1 engages Notch receptors on CD4^{+} T cells to promote mixed T_H2 and T_H17 cell-dependent inflammation. Antibody-mediated inhibition of the Notch receptors pointed to Notch4 as the critical Notch receptor involved in this pathway[8]. The identity of the CD4^{+} T cell subpopulation(s) expressing Notch4, the signals that regulate its induction and its downstream effector pathways remained unknown. Here, we identify Notch4 as a master molecular switch that subverts lung tissue T_{reg} cell function to promote allergic airway inflammation. Notch4 is mainly induced on allergen-specific induced (i)T_{reg} cells in an allergen and interleukin-6 (IL-6)-dependent manner, and acts to disrupt their function by Wnt and Hippo pathway-dependent mechanisms. Importantly, Notch4 acts via the Wnt pathway to induce the expression in lung tissue T_{reg} cells of the cytokine growth and differentiation factor 15 (GDF15). The latter is a cytokine previously implicated in metabolic adaption to inflammation[9, 10], which we show here to upregulate allergic tissue inflammation by directly activating group 2 innate lymphoid cells (ILC2). These findings place Notch4 at the intersection of allergen and pollutant-driven airway inflammation and suggest novel intervention strategies targeting Notch4 to restore long-term immune tolerance in asthma and related disorders.

Results

Notch4 is inducibly expressed on T_{reg} cells in allergic airway inflammation.

We determined by real time (RT-)PCR the identity of the Notch receptor species expressed in lung tissue T_{reg} and T_{eff} cells isolated from sham (PBS) and ovalbumin (OVA)-sensitized mice following their challenge with OVA, and from OVA-sensitized mice co-treated with intranasal UFP during the OVA challenge phase (OVA+UFP). *Notch4* transcript expression

was enriched in lung T_{reg} cells at baseline as compared to T_{eff} cells, and was sharply upregulated in OVA and especially OVA+UFP treated mice relative to *Notch1–3* species (Fig. 1a). These results were corroborated by flow cytometric analysis of the expression of respective Notch receptors in T_{reg} and T_{eff} cells, which confirmed the differential upregulation of Notch4 on lung T_{reg} cells in allergic airway inflammation (Fig. 1b,c; Extended Data Fig. 1).

To examine the signals driving the induction of Notch4 on iT_{reg} cells, we employed an *in vitro* iT_{reg} cell differentiation system in which naive $CD4^+$ T cells expressing the OT-II T cell receptor (TCR), specific for the $OVA_{323–339}$ peptide were incubated with $OVA_{323–339}$-pulsed primary alveolar macrophages (AM)[8]. The latter cell type potently drives iT_{reg} cell differentiation under non-inflammatory conditions, and at the same time critically promotes allergic airway inflammation by allergens and UFP by virtue of their inducible expression of Notch ligands, most notably Jag1[8]. Results revealed a stepwise increase in Notch4 expression in differentiating iT_{reg} cells in co-cultures with $OVA_{323–339}$- and $OVA_{323–339}$+UFP-pulsed AM (Fig. 1d). Addition of IL-6 to the cell cultures, but not IL-1β, tumor necrosis factor (TNF), IL-25 and Thymic Stromal Lymphopoietin (TSLP), resulted in super-induction of Notch4 expression on differentiating iT_{reg} cells in an antigen-dependent manner. IL-33 treatment did not induce Notch4 on its own, but augmented the expression of Notch4 induced by IL-6 (Fig. 1d; Extended Data Fig. 1). In contrast, treatment with an anti-IL-6 receptor (IL-6R) monoclonal antibody (mAb) suppressed Notch4 expression induced by $OVA_{323–339}$- and $OVA_{323–339}$+UFP-pulsed AM. Notch4 differentially localized in the *de novo* induced lung T_{reg} (iT_{reg}) cells as evidenced by their lack of Helios expression (Helios$^-$ T_{reg} cells) (Fig. 1e). Furthermore, in an antigen presenting cell-free system of *in vitro* iT_{reg} cell differentiation by treatment of naive T cells with anti-CD3+anti-CD28 mAbs in the presence of transforming growth factor beta 1 (TGF-β1)[11], addition of IL-6 to the cell culture induced Notch4 on differentiating T_{reg} cells, which was attenuated by T_{reg} cell-specific deletion of IL-6R alpha chain or the downstream transcription factor STAT3 using a *Foxp3*-driven Cre recombinase and floxed target alleles (*Foxp3*^{YFPCre}*Il6ra*$^{/}$ and *Foxp3*^{YFPCre}*Stat3*$^{/}$, respectively) (Fig. 1f). Chromatin immunoprecipitation confirmed IL-6-dependent STAT3 binding to the *Notch4* promoter in T_{reg} cells, but not to those of *Notch1*, *Notch2* or *Notch3* (Fig. 1g; Extended Data Fig. 1). These results identified IL-6 is a key inducer of Notch4 expression on differentiating allergen-specific lung tissue iT_{reg} cells.

Notch4 subverts T_{reg} cell-mediated immune tolerance in allergic airway inflammation.

To elucidate the pathogenic role of inducible Notch4 expression on lung T cells in allergic airway inflammation, we employed *CD4*^{Cre}*Notch4*$^{/}$ mice, in which a floxed *Notch4* allele is specifically deleted in all T cells (Extended Data Fig. 2a). Results showed that deletion of *Notch4* in $CD4^+$ T cells greatly attenuated airway inflammation induced in OVA-sensitized and challenged mice, without or with UFP treatment (Fig. 2a,b). *Notch4* deletion largely suppressed the increase in airway hyper-responsiveness (AHR) induced by OVA, and its super induction by UFP co-treatment (Fig. 2c). Because Notch4 is preferentially induced in T_{reg} cells in allergic airway inflammation, we employed *Foxp3*^{YFPCre}*Notch4*$^{/}$ mice, in which the floxed *Notch4* allele is specifically deleted in T_{reg} but not in T_{eff} cells, leading to the complete selective loss of Notch4 expression in the latter cells (Extended Data Fig. 2a,b).

The attenuated allergic airway inflammation noted in $CD4^{Cre}Notch4^{/}$ mice was completely reproduced in $Foxp3^{YFPCre}Notch4^{/}$ mice, indicating that the effect of Notch4 deletion is localized to T_{reg} but not to T_{eff} cells (Fig. 2a–c). $Notch4$ deletion in CD4$^+$ T cells or specifically in T_{reg} cells suppressed total and OVA-specific IgE responses, and T cell and eosinophil infiltration of lung tissues (Fig. 2d–g). $Notch4$ deletion also suppressed lung tissue T_H2 and T_H17 cell responses and reversed the destabilization of lung tissue T_{reg} cells towards T_H2 and T_H17 cell-like phenotypes, while keeping the T_{eff} and T_{reg} cell IFN-γ response unaltered (Fig. 2h,i; Extended Data Fig. 2c).

To assess the disease suppressive capacities of allergen-specific iT_{reg} cells that are lacking in Notch4 expression, we used an adoptive transfer model in which iTreg cells were derived in $vitro$ from naive splenic CD4$^+$ T cells of $Foxp3^{YFPCre}$ and $Foxp3^{YFPCre}Notch4^{/}$ mice that concurrently expressed the OTII transgene. The cells were adoptively transferred into OVA-sensitized $Foxp3^{YFPCre}$ mice, which were then challenged with aerosolized OVA and analyzed (Extended Data Fig. 2e–f). OTII$^+$ Notch4-deficient iT_{reg} cells were superior to their Notch4-sufficient counterparts in suppressing the different attributes of OVA-induced airway inflammation, including AHR, tissue eosinophilia and lymphocytosis in the lungs of the recipient mice. They were also superior in suppressing IL-4, IL-13 and IL-17 expression in the recipient lung T_{eff} and T_{reg} cells.

The salutary effects of $Notch4$ deletion on allergic airway inflammation was fully reproduced by T_{reg} cell-specific deletion of $Pofut1$, encoding an enzyme that mediates o-fucosylation of Notch receptors, a requisite event in their glycosylation modification that is essential to their function (Extended Data Fig. 3)[12, 13]. To determine the role of the canonical versus non-canonical pathways in mediating the effects of Notch signaling on T_{reg} cells in airway inflammation, we examined the impact of T_{reg} cell-specific deletion of $Rbpj$, encoding the canonical Notch adaptor RBPJ, on airway responses[13, 14]. Results revealed that $Foxp3^{YFPCre}Rpbj^{/}$ mice exhibited decreased AHR and tissue eosinophilia in-between those of $Foxp3^{YFPCre}Pofut1^{/}$ and $Foxp3^{YFPCre}$ mice (Extended Data Fig. 3). However, whereas the T_H2 cell responses were suppressed, the T_H17 cell responses were unaffected, indicating that the latter proceeds by a Notch non-canonical pathway. In contrast, T_{reg} cell-specific deletion of floxed $Notch1$ or $Notch2$ alleles, or global deletion of $Notch3$, had no impact on allergic airway inflammation (Extended Data Fig. 4).

The relationship between Notch4 expression in T_{reg} cells and airway inflammation was also investigated by interrupting upstream pathways regulating its expression. T_{reg} cell-specific deletion of $Il6r$a or $Stat3$ recapitulated the protective effect of T_{reg} cell Notch4 deficiency. Both deletions attenuated OVA-induced allergic airway inflammation, with decreased AHR, airway eosinophilia, total and OVA specific IgE, and T_H2 and T_H17 cell responses (Extended Data Fig. 5).

T_{reg} cell-specific $Notch4$ deletion was also found to be similarly protective across different aeroallergens. Thus, in a house-dust mite-induced model of allergic airway inflammation, it also suppressed airway inflammation and AHR, tissue eosinophilia and neutrophilia and T_H2/T_H17 cell responses (Extended Data Fig. 6). It was also protective in a chronic model of allergic airway inflammation in which, in addition to suppressing the inflammatory and

allergic responses noted above, it also suppressed sub-epithelial collagen deposition, a hallmark of airway remodeling due to chronic inflammation (Extended Data Fig. 7)[15]. Altogether, these results highlighted the critical role of IL6-STAT3-dependent Notch4 signaling pathways in the destabilization and dysregulation of lung T_{reg} cells in allergic airway inflammation.

Notch4 activates the Hippo and Wnt pathways to disrupt T_{reg} cell functions.

To further investigate the mechanisms by which Notch4 disrupted T_{reg} cell function, we analyzed the transcriptional profiles of T_{reg} cells isolated from the lungs of sham and OVA +UFP treated *Foxp3*[YFPCre] and *Foxp3*[YFPCre]*Notch4* / mice. Results revealed a Notch4-dependent dysregulation of several pathways in OVA+UFP treated mice previously shown to impact T_{reg} cell stability and/or function, with particularly prominent changes in the Hippo (*Wwtr1, Yap1, Tead1, Tead2, Tead3, Tead 4, Foxo6*)[16, 17], and Wnt pathways (*Ctnnb1, Serpine1, Fzd5,8,10* and *Wnt4,5a,8a,9a,9b,11*)[18, 19] (Fig. 3a,b; Data set 1). Notch4-dependent upregulation of the Hippo and Wnt pathways was confirmed by flow cytometry, which revealed increased expression of the Hippo pathway effector Yap, encoded by *Yap1*, and the Wnt pathway β-catenin, encoded by *Ctnnb1*, in lung T_{reg} cells in OVA and OVA +UFP-driven allergic airway inflammation. This increase was sharply downregulated upon T_{reg} cell-specific *Notch4* deletion (Fig. 3c,d). The regulation of the Hippo pathway by Notch4 was further investigated by analyzing the phosphorylation of the Hippo pathway intermediates Mob1 and Lats1 in lung T_{reg} cells of sham and OVA+UFP treated *Foxp3*[YFPCre] and *Foxp3*[YFPCre]*Notch4* / mice. *Notch4* deletion upregulated the phosphorylation of Mob1 and Lats1, which is consistent with dampening Hippo pathway activation by promoting Lats1/2 kinase-dependent proteolysis of the effector proteins Yap and Taz. These results indicate that Notch4 activates Hippo-dependent transcription by silencing its kinase cascade (Fig. 3e,f).

To determine the role of the Hippo and Wnt pathways in mediating T_{reg} cell subversion by Notch4, we examined the consequences of T_{reg} cell-specific deletion of genes encoding key components of the respective pathways on allergic airway inflammation induced by OVA +UFP. Combined T_{reg} cell-specific deletion of *Yap1* and *Wwtr1*, encoding the Hippo pathway transcriptional regulators Yap and Taz respectively[20], partially attenuated inflammation and AHR, whereas T_{reg} cell-specific deletion of *Ctnnb1*, encoding β-catenin[21], largely recapitulated the effect of T_{reg} cell-specific *Notch4* deletion in suppressing those parameters, with neither deletion affecting Notch4 expression (Fig. 4a–h). *Yap1* and *Wwtr1* deletion suppressed T_H17 and, to a lesser extent, T_H2 cell responses in the airways while upregulating T_H1 cell responses (Fig. 4a–d). In contrast, *Ctnnb1* deletion profoundly suppressed the T_H2 cell-like reprogramming of Notch4^{hi} T_{reg} cells and the airway conventional T_H2 cell response but left the T_H17 cell responses unaffected (Fig. 4e–h). Combined deletion of *Yap1, Wwtr1* and *Ctnnb1* in Treg cells reproduced the full effect of *Notch4* deletion in suppressing allergic airway inflammation and T_H2 and T_H17 responses (Fig. 4i,j). These results indicated that the Hippo and Wnt pathways mediated distinct, complementary aspects of Notch4 signaling in disrupting immune tolerance in allergen and pollutant-induced allergic airway inflammation.

Notch4 promotes T$_{reg}$ cell destabilization towards T$_H$2 and T$_H$17 cell fates.

To determine whether Notch4 acted to destabilize lung T$_{reg}$ cells to give rise to Foxp3$^-$ T$_H$2 and T$_H$17 ex-T$_{reg}$ cells, we employed a lineage tracing approach using a *Rosa26* Stop-flox EGFP reporter (*R26*^{EGFP}) crossed to *Foxp*^{YFPCre}. *Foxp3*^{YFPCre}*Notch4*$^{/}$ *R26*^{EGFP} and control *Foxp3*^{YFPCre}*R26*^{EGFP} mice were either sham or OVA sensitized and then challenged with aerosolized OVA without or with intranasal UFP treatment. Cytokine expression was examined in T$_{reg}$ (YFP$^+$EGFP$^+$), ex-T$_{reg}$ (YFP$^-$EGFP$^+$) and CD4$^+$ T$_{eff}$ cells (YFP$^-$EGFP$^-$). The frequencies of YFP$^-$EGFP$^+$ ex-T$_{reg}$ cells were markedly increased in the lungs of *Foxp3*^{YFPCre}*R26*^{EGFP} OVA sensitized and challenged group, and were further increased in the OVA+UFP treated group, with the exT$_{reg}$ cells reaching up to a third of the total T$_{reg}$ lineage-derived (EGFP$^+$) cells in the lung (Fig. 5a). In contrast, the ex-T$_{reg}$ cells were markedly decreased in the equivalent *Foxp3*^{YFPCre}*Notch4*$^{/}$ *R26*^{EGFP} groups, indicative of heightened T$_{reg}$ cell instability mediated by Notch4 (Fig. 5a). Approximately half of the ex-T$_{reg}$ cells were T$_H$2 and T$_H$17-skewed cells at a ratio of 3:1, with both being suppressed in *Foxp3*^{YFPCre}*Notch4*$^{/}$ *R26*^{EGFP} mice (Fig. 5b,c).

To investigate the source of Notch4-mediated T$_{reg}$ cell instability, we further examined the epigenetic methylation signature of the *Foxp3* CNS2 promoter region, which inversely affects T$_{reg}$ cell lineage stability[22, 23]. There was increased methylation of the CpG elements in the *Foxp3* CNS2 of T$_{reg}$ cells isolated from the lungs of OVA+UFP-treated mice as compared to those of sham treated mice, which segregated with high but not low Notch4 expression (Notch4^{hi} versus Notch4^{lo}) (Fig. 5d,e). Increased CNS2 CpG methylation was also reversed upon T$_{reg}$ cell-specific deletion of *Notch4* compared to that of total lung T$_{reg}$ cells of *Foxp3*^{YFPCre} control mice. Combined *Yap1* and *Wwtr1* but not *Ctnnb1* deletion fully reversed the increased methylation of the *Foxp3* CNS2 in lung T$_{reg}$ cells of OVA/UFP-treated mice, indicating that the destabilization of T$_{reg}$ cells by Notch4 signaling was mediated by the Hippo but not by the Wnt pathway (Fig. 5d,e).

We also investigated the role of Notch4 expression in impairing T$_{reg}$ cell function by sorting out Notch4^{hi} versus Notch4^{lo} T$_{reg}$ cells from the lungs of *Foxp3*^{YFPCre} OVA+UFP treated group as well as T$_{reg}$ cells from untreated control *Foxp3*^{YFPCre} mice and examining these three groups of T$_{reg}$ cells for their suppressive capacity. Whereas the Notch4^{lo} lung T$_{reg}$ cells from OVA+UFP treated mice were equivalent to control lung T$_{reg}$ cells in their capacity to inhibit *in vitro* T cell proliferation, the suppressive function of Notch4^{hi} lung T$_{reg}$ cells was profoundly impaired (Fig. 5f). Combined *Yap1* and *Wwtr1* but not *Ctnnb1* deletion fully restored the in vitro suppressive function of Notch4^{hi} T$_{reg}$ cells, consistent with the impact of the respective pathways on CNS2 demethylation (Fig. 5g,h). Overall, these results indicated that Notch4 induced T$_{reg}$ cell instability and T$_H$2 and T$_H$17-cell-like reprogramming in the context of allergic airway inflammation, and that this destabilization was associated with epigenetic methylation at the *Foxp3* CNS2 locus mediated by the Hippo pathway.

A T$_{reg}$ cell Notch4-Wnt-GDF15 pathway promotes ILC2 expansion and activation.

ILC2 play a key role in allergic airway inflammation by virtue of copious secretion of type 2 cytokines, most prominently IL-13[24]. Total ILC2 as well as IL-13-expressing ILC2 were

sharply increased in OVA and especially OVA+UFP-treated mice but were dramatically reduced upon deletion of *Notch4* in T_{reg} cells (Fig. 6a). The effect of T_{reg} cell-specific *Notch4* deletion on ILC2 expansion and activation was reproduced by *Ctnnb1* but not *Yap1 and Wwtr1* T_{reg} cell-specific deletion (Fig. 6a). *In vitro* studies revealed that Notch4^{hi} T_{reg} cells derived from OVA+UFP-treated *Foxp3*^{YFPCre} mice failed to suppress the upregulation of IL-13 expression in ILC2 derived from the inflamed lungs of the same mice (Fig. 6b). In contrast, Notch4^{lo} lung T_{reg} cells derived from the OVA+UFP-treated *Foxp3*^{YFPCre} mice or Notch4-deficient T_{reg} cells derived from OVA+UFP-treated *Foxp3*^{YFPCre}*Notch*4$^{/}$ mice potently suppressed IL-13 expression, as did treatment of Notch4^{hi} T_{reg} cells with an anti-Notch4 mAb (Fig. 6b). Further analysis revealed that T_{reg} cell-specific *Ctnnb1* but not Yap and Taz deletion restored the ILC2 suppressive function of Notch4^{hi} T_{reg} cells, thus implicating the Wnt pathway in the failure of ILC2 regulation (Fig. 6c).

RNA-seq analysis identified *Gdf15* transcripts to be highly enriched in lung T_{reg} cells of OVA+UFP-treated *Foxp3*^{YFPCre} mice. (Fig. 3a). Consistent with this finding, transcripts encoding the cytokine GDF15 were highly induced in Notch4^{hi} lung T_{reg} cell in a β-catenin-dependent manner (Fig. 6d). Flow cytometric analysis confirmed that T_{reg} cells were the primary source of GDF15 in the inflamed lungs of OVA and OVA+UFP treated mice, whereas GDF15 was sharply downregulated in Notch4- and β-catenin-deficient, but not Yap/Taz-deficient, T_{reg} cells (Fig. 6e). Addition of recombinant GDF15 to *in vitro* cultures of ILC2 derived from naive mice upregulated IL-13 expression alone and especially in synergy with IL-33 (Fig. 6f). Furthermore, the *in vitro* co-culture of GDF15-expressing Notch4^{hi} T_{reg} cells, isolated from lungs of OVA+UFP-treated mice, with naive ILC2 cells upregulated the expression of IL-13 in the latter, an effect that was reversed by the addition of a GDF15 blocking peptide (Fig. 6g). Addition of GDF15 blocking peptide restored the ILC2 suppressive function of lung T_{reg} cells of OVA+UFP-treated mice, consistent with the critical role of the Wnt-GDF15 axis in the failure of ILC2 regulation (Fig. 6h).

The contribution of GDF15 to the allergic airway inflammatory response was explored by intra-tracheal instillation of recombinant GDF15 in OVA+UFP-treated *Foxp3*^{YFPCre}*Notch4*$^{/}$ mice, which resulted in the upregulation of AHR and tissue inflammation, as well as the increased expression of IL-4 and IL-13 in T_{eff} cells (Fig. 7a–c). Reciprocally, instillation of the GDF15 blocking peptide suppressed the aforementioned changes in OVA+UFP treated *Foxp3*^{YFPCre} mice (Fig. 7d–f). The essential role of ILC2-derived IL-13 in mediating the effects of GDF15 on airway inflammation was established by specifically deleting an *Il4-Il13* gene cassette in ILC2 using a *Rora*-driven Cre recombinase (*Rora*^{Cre}*Il4*$^{/}$*Il13*$^{/}$). ILC2-specific deletion of *Il4-Il13* reduced OVA+UFP-driven airway inflammation, and abrogated the capacity of GDF15 to further upregulate it. GDF15 treatment did not affect the expression of IL-13 in T_{eff} cells neither in control *Rora*^{Cre} mice nor in *Rora*^{Cre}*Il4*$^{/}$*Il13*$^{/}$ (Fig. 7g,h). Overall, these findings confirmed that Notch4 expression abrogated the capacity of lung T_{reg} cells to suppress ILC2 and activated a T_{reg} cell-intrinsic Wnt-GDF15 axis that promoted ILC2 activation.

T$_{reg}$ cell Notch4 expression segregates with disease severity in asthmatics.

To determine the relevance of the Notch4 signaling pathways in human subjects with asthma, we analyzed the expression of Notch4 on peripheral blood mononuclear cells (PBMC) of asthmatic and control subjects (demographics, disease severity classification of asthmatic subjects are described in Supplementary Table 1. Results revealed that asthmatics had elevated frequencies of circulating Notch4^{hi} T$_{reg}$ cells, with both the cell frequencies and expression intensity progressively increasing as a function of asthma severity, reaching up to 50% of circulating T$_{reg}$ cells in severe asthmatics (Fig. 8a). In contrast, Notch4 expression on circulating CD4$^+$ T$_{eff}$ cells was low and remained relatively low as a function of asthma severity (Fig. 8b). Increased expression of Notch4 in circulating T$_{reg}$ cells of asthmatics was found independent of the atopic status of patients (Extended Data Fig. 8). Also, expression of Notch1–3 on T$_{reg}$ and T$_{eff}$ cells was not increased in asthmatics as compared to control subjects (Extended Data Fig. 8). Subjects with other allergic diseases expressed Notch4 on their circulating T$_{reg}$ cells at levels that were either similar to those of controls (e.g food allergy) or equivalent to those of mild asthmatics (e.g. eczema without or with food allergy).

Further analysis revealed that Notch4 expression was restricted to the circulating Helios$^−$ iT$_{reg}$ cell subpopulation (Fig. 8c). T$_{reg}$ cell expression of the Hippo and Wnt pathway effector proteins Yap/Taz and β-catenin, respectively, localized to Notch4$^+$ T$_{reg}$ cells and similarly increased as a function of asthma severity (Fig. 8d,e). Also, there were increased concentrations of GDF15 in the sera of moderate and severe asthmatics that positively correlated with circulating T$_{reg}$ cell Notch4 expression, whereas those of mild asthmatics were similar to those of controls (Fig. 8f and Extended Data Fig. 8). The contribution of Notch4 signaling to T$_{reg}$ cell dysfunction was ascertained by the demonstration that Notch4^{hi} peripheral blood T$_{reg}$ cells poorly suppressed *in vitro* T cell proliferation as compared to Notch4^{lo} T$_{reg}$ cells isolated from the same asthmatic subjects or to T$_{reg}$ cells isolated from healthy control subjects, which were overwhelmingly Notch4^{lo} (Fig. 8g). Moreover, the *in vitro* co-culture of Notch4^{hi} T$_{reg}$ cells, isolated from peripheral blood of severe asthmatics, failed to suppress the activation of ILC2 cells compared to T$_{reg}$ cells of healthy control subjects, a defect that was reversed by the addition of a GDF15 blocking peptide (Fig. 8h).

Analysis of peripheral blood cells of a severe asthmatic subject treated with the anti-IL-6R mAb Tocilizumab revealed decreased Notch4 expression on the patient T$_{reg}$ cells post initiation of therapy, consistent with the requirement for IL-6R signaling to upregulate Notch4 expression (Fig. 8i)[25]. These results, which mirror those obtained in the mouse system, indicate that Notch4 expression may similarly serve as an immune regulatory switch that licenses allergic inflammation in human asthmatics.

Discussion

In this study, we have identified a novel pathway central to the pathogenesis of asthmatic airway inflammation involving the inducible expression of Notch4 on allergen-specific T$_{reg}$ cells. This induction, synergistically mediated by allergens and ambient pollutant particles, activates downstream Hippo and Wnt pathways to subvert T$_{reg}$ cell stability and functions.

Inhibition of Notch4 expression in T_{reg} cells, but not that of other Notch receptors, suppressed airway inflammation and restored immune tolerance. Critically, Notch4 signaling upregulated the expression in T_{reg} cells of GDF15, a cytokine that we demonstrate to reinforce airway inflammation by a novel mechanism involving ILC2 activation. Notch4 and its downstream effector pathways were upregulated on T_{reg} cells of asthmatic subjects as a function of disease severity, thus identifying Notch4 as an immune regulatory switch mechanism that licenses asthmatic inflammation and highlighting the therapeutic potential for tolerance restoration in asthma.

Induction of Notch4 on T_{reg} cells in the airway involved coordinate allergen peptide-specific TCR activation and IL-6-STAT3 signaling, a process further upregulated by IL-33. Remarkably, this pathway thus integrates several genetic loci, including *NOTCH4*, *IL6* and *IL33*, identified to impart susceptibility to asthma incidence and/or disease severity[26, 27, 28, 29, 30]. T_{reg} cell-specific deletion of *Il6ra* or *Stat3* substantially attenuated Notch4 expression in T_{reg} cells in allergic airway inflammation, as did treatment of a severe asthmatic subject with the anti-IL-6Rα chain mAb tocilizumab[25]. STAT3 was demonstrated to bind to the *Notch4* promoter, consistent with direct upregulation of Notch4 expression by IL-6-STAT3 signaling. The specificity of Notch4 induction on lung T_{reg} cells may relate to a "niche effect", in which the interaction with alveolar macrophages normally drives differentiation of naive allergen specific T cells into T_{reg} cells[8, 31]. The uptake of allergens and ambient particulate matter is associated with the production of IL-6 and upregulation of Notch ligands including Jag1[8], driving T_{reg} skewing towards T_{eff} cell phenotypes in a Notch4-dependent manner.

Notch4 expression on lung T_{reg} cells mobilized several downstream pathways, notably Hippo and Wnt, to derail T_{reg} cell stability and function. Expression of effectors of both pathways, including Yap and Taz (Hippo) and β-catenin (Wnt) also segregated with Notch4 expression in peripheral blood T_{reg} cells of human asthmatics and correlated with asthma severity. The two pathways acted to disrupt different aspects of T_{reg} cell functions. Whereas the Hippo pathway impaired lung T_{reg} cell *in vitro* suppressor function and promoted their skewing towards the T_H17 cell fate, the Wnt pathway promoted their T_H2 cell-like reprogramming and was essential to the T_H2 effector T cell response in the airways. T_{reg} cell specific deletion of *Rbpj* segregated the T_H2 and T_H17 responses along the canonical and non-canonical pathways, respectively. Thus, Notch4 mobilizes distinct signaling pathways within lung T_{reg} cells that act in a modular fashion to disrupt immune tolerance in the airways.

An important pathogenic mechanism mobilized by Notch4 is the potentiation of ILC2 activation, which proceeded by a T_{reg} cell-intrinsic, β–catenin-dependent pathway. Notch4-β-catenin signaling impaired the suppression by T_{reg} cells of activated ILC2. Furthermore, it positively promoted the activation of resting ILC2 by inducing the expression in T_{reg} cells of GDF15, which selectively activated ILC2 but not T cells in synergy with IL-33. Antagonism of GDF15 augmented the *in vitro* suppression of ILC2 by Notch4^{hi} T_{reg} cells and down-regulated airway inflammation *in vivo*. These results indicated a critical role for GDF15 in mediating an ILC2-dependent forward amplificatory loop by which Notch4^{hi} T_{reg} cells actively promote asthmatic inflammation.

Analysis of Notch4 expression on circulating T_{reg} cells of a pediatric cohort of asthmatic subjects demonstrated a step-wise increase in Notch4 expression as a function of asthma severity, with the T_{reg} cells of severe asthmatics especially marked by high expression of Notch4 and its downstream effectors Yap, Taz and β-catenin. Similar to the mouse studies, Notch4-expressing human T_{reg} cells also showed impaired *in vitro* suppressive function. Remarkably, there was minimal heterogeneity in Notch4 expression within each disease severity subgroup, highlighting Notch4 as a common pathogenic mechanism operative in these patients whose amplitude is highly informative of disease activity. These results emphasize the potential usefulness of Notch4 and its down-stream Hippo and Wnt effectors as novel biomarkers to monitor disease activity and response to therapy.

In conclusion, our studies identify a novel mechanism central to the pathogenesis of asthmatic inflammation. These studies, together with earlier ones on the role of Notch1 expression on T_{reg} cell in promoting T_H1 cell inflammatory and autoimmune responses[13, 32], hint at a T_{reg} cell-specific Notch receptor code that directs different T_H cell- responses in allergic and autoimmune diseases. Elucidating the respective roles of different Notch receptors in controlling disease outcome by modulating T_{reg} cell responses may offer opportunities for precision medicine interventions to restore immune tolerance in a tissue and disease-specific manner.

Methods

Mice.

The following mouse strains were obtained from the JAX Laboratories: *CD4*[Cre] (B6.Cg-Tg(Cd4-cre)1Cwi/BfluJ)[33], floxed *Ctnnb1* (*Ctnnb1*^{fl/fl}) (B6(Cg)-*Ctnnb1*[tm1Knw]/J)[34], *Foxp3*[YFPCre] (B6.129(Cg)-*Foxp3*[tm4(YFP/icre)Ayr]/J)[35], *Il6i*^{fl/fl} (B6;SJL-*Il6ra*[tm1.1Drew]/J)[36], *Notch1*^{fl/fl} (B6.129X1-*Notch1*[tm2Rko/Grid]/J)[37], *Notch2*^{fl/fl} (B6.129S-*Notch2*[tm3Grid]/J)[38], *Notch3*^{−/−} (B6;129S1-*Notch3*[tm1Grid]/J)[39], OT-II (B6.Cg-Tg($T_{cra}T_{crb}$)425Cbn/J)[40], Stat3^{fl/fl} (B6.129S1-*Stat3*[tm1Xyfu]/J)[41], *Wwtr1*^{fl/fl} (B6.129(Cg)- *Wwtr1*[tm1Hmc]/J) and *Yap1*^{fl/fl} (B6.129P2(Cg)- *Yap1*[tm1.1Dupa]/J)[42, 43], and CD45.1 (B6.SJL-*Ptprc*[a] *Pepc*[b]/BoyJ) mice. Notch4^{fl/fl} (*Notch4*[tm1c(NCOM)Mfgc]) were obtained from the Canadian mutant mouse repository. *Pofut1*^{fl/fl} (B6.Cg-Pofut1[tm2.1Pst]/J), *Rbpj1*^{fl/fl} (B6.129P2-*Rbpj*[tm1Hon]/HonRbrc) were kind gifts of Pamela Stanley and Tasuku Honjo, respectively[12, 14].

Particles.

UFP (0.18 μm) were collected in an urban area of downtown Los Angeles, as previously reported[7]. The respective particles were suspended in an aqueous solution, with the hydrophilic components becoming part of the solution, while the solid non-soluble UFP cores are left in suspension. The entire mixture was administered intranasally, as indicated below.

T cell co-cultures with lung alveolar macrophages.

Naïve CD4^{+}OTII^{+} T cells were isolated from spleens of *OTII*^{+}*Foxp3*[YFPCre] mice by fluorescein-activated cell sorting (FACS). AM were isolated by flowcytometry as shown in[8], and were aliquoted at 2×10^4 cells in 48 well plates, then either sham treated, treated

overnight with $OVA_{323-339}$ or with $OVA_{323-339}$ and UFP at 10 µg/ml. The treated AMs were washed twice with PBS to remove residual UFP, and the $OTII^+$ naïve $CD4^+$ T cells were then added at 4×10^5 cells/well in a final volume of 0.5 ml 10% fetal calf serum (FCS)/RPMI culture medium. Recombinant IL-1β, IL-25, TSLP, and TNFα (Peprotech) were added at a concentration of 10 µg/ml. Recombinant IL-6 and IL-33 (Peprotech) were titrated from 10 µg/ml to 1 µg/ml. Rat anti-mouse IL-6 mAb (clone: MP5–20F3, Bioxcell) was added at a concentration of 10 µg/ml.

In vitro iT$_{reg}$ cell differentiation.

Sorted naïve $CD4^+CD62L^+Foxp3^{YFPCre}$ T cells (1×10^6/ml) were cultured with plate-bound anti-CD28 (5 µg/ml, Biolegend), anti-CD3 (clone: 145–2C11, 5 µg/ml, Biolegend), recombinant TGF-β1 (5 ng/ml, R&D Systems), with or without IL-4 (10 ng/ml) (Peprotech), anti-IL-4 (clone: 11B11, 10 µg/ml) (Biolegend) or anti-IL-6 mAb (MP5–20F3, 10 µg/ml) (Biolegend), mitogen activated protein kinase (MEK) inhibitor PD98059 (50 µM, Sigma-Aldrich) or P38 inhibitor IV (10 µM, Sigma-Aldrich). After 4 days, the induced T$_{reg}$ cells were analyzed by flow cytometry for Foxp3 expression and intracellular cytokines production and/ re-sorted on the basis of YFP expression.

In vitro suppression assays.

Total $CD4^+$ T cells were isolated using a CD4 negative isolation kit (Miltenyi Biotec) followed by cell sorting on FACSAria. Isolated T$_{eff}$ cells were labeled with CellTrace Violet Cell Proliferation dye according to the manufacturer's instructions (Life Technologies) and were used as responder cells. T$_{reg}$ cells were isolated on a FACSAria on the basis of CD4, YFP and/or Notch4 expression and were used as suppressor cells. Responder cells were co-cultured with T$_{reg}$ cells, at the indicated ratios, and stimulated for 3 days with 2 µg/ml of coated anti-CD3 and 5 µg/ml of soluble anti-CD28 in 96-well, round-bottomed plates in triplicates. The responder cells (YFP^- were then analyzed for CellTrace dye dilution by flow cytometry. For our human suppression assay studies, T$_{reg}$ cells were isolated on the basis of $CD4^+CD25^+CD127^-$ (T$_{reg}$) while Teff cells were isolated as $CD4^+CD25^-CD127^+$ (T$_{eff}$) from either healthy controls or severe asthmatics. T$_{eff}$ cells were then stained with Cell Trace Violet Cell Proliferation dye (Invitrogen) and platted in a concentration of 10^4 cells in a U-bottom 96 well plate with 0.1µL prewashed T cell activation and Expansion beads (Thermofischer) in 100µL complete medium. Different numbers of T$_{reg}$ cells are added to the culture in 100µL of complete medium in order to have 1/1, 1/2, 1/4 and 1/8 ratios (respectively 10^4, $5X10^3$, $2.5X10^3$, $1.25X10^3$ cells) or 100µL of complete medium for wells without T$_{reg}$ cells. The cultures will be incubated at 37°C 5% CO_2 for 4 days. On the fourth day, the cells will be stained again for CD4, CD127 and CD25 and evaluate the dilution of the proliferation dye by gating on $CD4^+ CD127^+Violet Tracer^+$ cells.

In vitro ILC2 suppression assay.

Innate lymphoid cells (ILC) were isolated from lungs of OVA+UFP sensitized, challenged and treated mice. ILC2 were isolated as Lineage (Lin)$^-$ (CD3, CD4, CD11c, CD11b, CD19, SiglecF, F4/80)$^-$Thy1.1$^+$Sca-1$^+$ T1/ST2$^+$. IL-13 percentages were checked at the beginning of the experiment. ILC2 were then co-cultured with 10^5 cells/well. T$_{reg}$ cells at these different concentrations, 1:5, 1:10 or 1:20, from $Foxp3^{YFPCre}$ mice either sham treated or

treated OVA+UFP with high Notch4 expression with or without the addition of anti-Notch4 mAb (clone: HMN4–14, Bioxcell) in concentration of 10ng/ml, T_{reg} cells from $Foxp3^{YFPCre}Notch4^{/}$, $Foxp3^{YFPCre}Ctnnb1^{/}$ or $Foxp3^{YFPCre}Yap1^{/} Wwtr1^{/}$ mice treated with OVA+UFP. 48 hours later, IL-13 expression of ILC2 was measured by flowcytometric analysis.

In vitro ILC2–T_{reg} cell co-cultures.

ILC2 cells were isolated from the lungs of naïve Foxp3[YFPCre] mice. These cells were incubated with either IL-33 (10 μg/ml), Notch4^{high} T_{reg} cells isolated from the lungs of OVA +UFP treated mice or with both along with or without GDF15 blocking peptide (Mybiosource) (10 ng/ml)[44]. 48 hours later, the expression of IL-13 in ILC2 cells was measured by flowcytometric analysis.

In vitro ILC2–GDF15 co-cultures.

ILC2 cells were isolated from the lungs of naïve Foxp3[YFPCre] mice. These cells were incubated with either IL-33 (10 μg/ml), recombinant GDF15 (R&D) (10 μg/ml) or both. 48 hours later, the expression of IL-13 in ILC2 cells was measured by flow cytometry.

Isolation of Human peripheral blood mononuclear cells (PBMCs).

Human PBMCs were isolated from full blood from either healthy control, mild asthmatics, moderate asthmatics or severe asthmatics probands via density gradient using Ficoll (GE Healthcare). PBMCs were then stored frozen in Fetal Calf Serum (FCS) (Sigma Aldrich) and 15% Dimethyl sulfoxide (DMSO) (Sigma Aldrich). The cells were later thawed for analysis of their Notch, Yap1 and -Catenin expression by flow cytometry.

Isolation, culture and suppression assay of Human peripheral ILC2 cells.

Human ILC2 cells were isolated used human ILC2 isolation kit (Miltenyi Biotec). The cells were then stained for CD294 and Lineage and sorted out as CD294^{+}Lineage^{−}. The ILC2 cells were then cultured with IL-33 (10 μg/ml) (Peprotech) and IL-25 (2 μg/ml) (Peprotech) for 5 days. Moreover, T_{reg} cells were isolated from either asthmatics or healthy controls by sorting them out as CD4^{+}CD25^{+}CD127^{−} cells. The T_{reg} cells were cultured with the ILC2 in a 1:5 or 1:10 with and without the addition of GDF15 blocking peptide. 48 hours later, the production of IL-13 by the ILC2 were assessed by flow cytometric analysis.

GDF15 ELISA.

EDTA Plasma from 88 probands (Control subjects, mild, moderate and severe persistent asthma patients) were used to measure GDF15 using enzyme-linked immunosorbent assay (ELISA) (R&D) according to manufacturer's protocol.

Allergic sensitization and challenge.

Mice were sensitized to OVA by intraperitoneal (i.p.) injection of 100 μg OVA in100 μl PBS, then boosted two weeks later with a second i.p. injection of OVA in PBS. Control mice were sham sensitized and boosted with PBS alone. Starting on day 29, both OVA and sham-sensitized mice were challenged with aerosolized OVA at 1%, for 30 minutes daily for 3

days. Two hours before each OVA aerosol exposure, subgroups of mice were given intranasally (i.n.) either PBS or UFP at 10 μg/100μl PBS/instillation. Mice were euthanized on day 32 post sensitization and analyzed. For dust mite-induced allergic airway inflammation, mice received 5 μg of lyophilized D. Pteronyssinus extract (Greer) in 100 μl PBS intranasally for 3 days at the start of the protocol then challenged with the same dose of D. Pteronyssinus extract on days 15–17 with or without UFP at the same concentration as before. Mice were euthanized on day 18 and analyzed for measures of airway inflammation. Bronchoalveolar lavage (BAL) fluid and lung tissues were obtained and analyzed for cellular components and T cell cytokine expression as described[6]. For the chronic model, Mice were sensitized to OVA by three intraperitoneal injections 10 mg OVA (Sigma) adsorbed to 1.5 mg Al(OH)3 (Pierce, Rockford) diluted in 200 mL phosphate-buffered saline (PBS)] on days 1, 14 and 21. The mice were challenged with OVA aerosol (1% wt/vol in PBS) via the airways twice a week on 2 consecutive days over a period of 12 weeks as previously described[15]. Sham sensitization and challenges were carried out with sterile Al(OH)3 in PBS. Animals were analyzed after 12 weeks of OVA aerosol challenge.

Measurement of airway functional responses.

Allergen-induced airway hyperreactivity (AHR) was measured, as previously described[8]. Anesthetized mice were exposed to doubling concentrations of aerosolized acetyl-β-methacholine (Sigma-Aldrich) by using a Buxco small-animal ventilator (Data Sciences International). The relative peak airway resistance for each methacholine dose, normalized to the saline baseline, was calculated.

Lung histopathology staining.

Paraffin-embedded lung sections were stained with hematoxylin and eosin (H&E) or Paraffin-acid-Schiff staining (PAS). The lung pathology was scored by blinded operators. Inflammation was scored separately for cellular infiltration around blood vessels and airways: 0, no infiltrates; 1, few inflammatory cells; 2, a ring of inflammatory cells 1 cell layer deep; 3, a ring of inflammatory cells 2–4 cells deep; 4, a ring of inflammatory cells of >4 cells deep[15]. A composite score was determined by the adding the inflammatory scores for both vessels and airways.

Polymerase Chain Reaction (PCR). B-cells

T_{reg} and/or T_{eff} cells were sorted out using ARIA II sorter (BD). mRNA isolation was conducted according to manufacturers' protocol (Qiagen). cDNA and qualitative PCR (qPCR) were performed using RT-PCR cDNA conversion kit (Qiagen) and probes for Notch1, Notch2, Notch3, Notch4 and GDF15 from applied biosystems (ThermoFisher). The mRNA expression was normalized to Notch1 expression in T_{eff} cell

Flow cytometric analysis of mouse and human cells.

Antibodies against the following murine antigens were used for flow cytometric analyses:

IL-4 (clone 11B11, catalogue no: 504104 1:300 dilution, Biolegend), Siglec-F (E50–2440, catalogue no: 5521261:300, BD Pharmingen), Foxp3 (FJK-16S, catalogue no: 48–5773-82 1:300, eBioscience), IFN-γ (XMG1.2, catalogue no: 505806 1:300, Biolegend), IL-13

(eBio13a, catalogue no.: 47–7133-82 1:300, eBioscience), Helios (22F6, catalogue no: 47–9883-42 1:200, eBioscience), CD11c (N418, catalogue no: 117318 1:500, Biolegend), CD11b (M1/70, catalogue no: 101222 1:500, eBioscience), CD4 (GK1.5, catalogue no: 100451, 1:500, Biolegend), CD3 (17A2, catalogue no: 100203, 1:500, Biolegend), IL-17 (TC11–18H10.1, catalogue no: 506922, 1:200, Biolegend), GR-1 (RB6–8C5, catalogue no: 108406, 1:500, Biolegend), CD45 (30-F11, catalogue no: 103140, 1:300, Biolegend), Notch1 (HMN1–12, catalogue no: 130615, 1:500, Biolegend), Notch2 (HMN2–35, catalogue no: 130714, 1:500, Biolegend), Notch3 (HMN3–133, catalogue no: 130512, 1:300, Biolegend), Notch4 (HMN4–14, catalogue no: 128407 1:200,Biolegend). Polyclonal rabbit anti-GDF15(catalogue no: 32572–05171, 1:200, Assaypro), anti-CD16/CD32 (clone: 93, Catalogue no: 101319, 1:1000, Biolegend), Alexa Fluor 647 goat anti-rabbit IgG Ab (clone PA5–39741, catalogue no: A32733, 1:1000, Thermofischer), p-Mob1 Ab (T35; clone D2F10, Catalogue no: 8699S, 1:300, CST), rabbit anti-mouse p-Lats1 Ab (T35; clone D57D3, 1:300, CST), rabbit anti-mouse p-Lats1/2 Ab (S909/872; clone PA5–39741, catalogue no: PA5–105895, 1:300, Thermofischer), Rat anti-mouse IL-6 mAb (Clone: MP5–20F3, Catalogue no: BE0046, 1:500, Bioxcell), anti-CD28 (Clone: 37.51, Catalogue no: 122004, ,1.1000, Biolegend) , anti-IL-4 (Catalogue no: 500-P54, 1:1000, Peprotech). Antibodies against the following human antigens were used: CD3 (HIT3a, catalogue no: 300318, 1:300,Biolegend), CD4 (RPA-T4, catalogue no: 300530, 1:300,Biolegend), Foxp3 (PCH-101,catalogue no: 48–4776-42 1:200, ebioscience), Helios (22F6, catalogue no: 47–9883-42 1:200, eBioscience), Notch1 (HMN1–519, catalogue no: 352108, 1:500, BD Pharmingen), Notch2 (HMN2–25, catalogue no: 742291, 1:300, BD Pharmingen), Notch3 (HMN3–21, catalogue no: 744828, 1:300, BD Pharmingen), Notch4 (HMN4–2, Catalogue no: 563269, 1:300, BD Pharmingen), Yap1 (147295, Catalogue no: 14729S, 1:200, CST) and beta-Catenin (196624, Catalogue no: IC13292V, 1:500,R&D system). The specificity and optimal dilution of each antibody was validated by testing on appropriate negative and positive controls or otherwise provided on the manufacturer's website. Intracellular cytokine staining was performed as previously described[13]. Furthermore, for YFP/GFP/cytokine staining, a different protocol was used. Cells were resuspended cells in approximately 100 μl 4% formaldehyde per 1 million cells for 15 min at room temperature (20–25°C). after centrifugation, the pellet was resuspended with 100 μl of Triton X for each 1 million cells. The mix was incubated at RT for 10 minutes. Cytokines were stained overnight as previously prescribed in[13]. Dead cells were routinely excluded from the analysis based on the staining of eFluor 780 Fixable Viability Dye (1:1000 dilution) (eBioscience). Stained cells were analyzed on a BD LSR Fortessa cell analyzer (BD Biosciences) and data were processed using Flowjo (Tree Star Inc.).

Chromatin Immunoprecipitation (ChIP).

For ChIP analysis, two systems were used. For STAT3 ChIP, iT$_{reg}$ cells were used after naïve T-cell differentiation protocol. These cells were stimulated with or without IL-6 at concentration of (10 μg/ml). Cells were then directly cross linked with 10% PFA for 8 min at room temperature (RT). Chromatin was then treated with lysis buffer I and lysis buffer II. ChIP protocol was conducted as described[45]. Quantitative PCR was conducted to measure enrichment percentage to input controls at the *Notch1* promoter region forward primer 5'-CACAAGGGGGGTAAGGGTTC-3'; reverse primer 5'-

GAGGCACTAGTGAGGCTCTGA-3', *Notch2* forward primer 5'-TTTCAAGCTCCTGCTGTCTCT-3'; reverse primer 5'-CTCTGGGCATTTCGTTCATT-3', *Notch3* forward primer 5'-AGGCTTGGCGGGTAGAAG-3'; reverse primer 5'-TCCCTCCTCCCTCTTTCC-3' and *Notch4* forward primer 5'-GCTCACAACCATCCGTAACA-3'; reverse primer 5'-ACTGAAACCGGTCACTTTGG-3' promoter regions.

DNA methylation.

The methylation status of the Foxp3 T_{reg} cell–specific demethylation region Conserved non-coding sequence 2, (CNS2) of *Foxp3*^{YFPcre}, *Foxp3*^{YFPcre}*Notch4*$^{/}$, *Foxp3*^{YFPcre}*Ctnnb1*$^{/}$ and *Foxp3*^{YFPcre}*Yap1*$^{/}$*Wwtr1*$^{/}$ lung T_{reg} cells of OVA+UFP mice were assessed. DNA extraction, bisulfite conversion, pyrosequencing, and data analysis were done by EpigenDx as published previously[46, 47]. twelve cytosine guanine dinucleotides (CpGs) of the mouse Treg-specific demethylation region (CNS2 of FOXP3) were analyzed.

Transcriptome Profiling.

T_{reg} cells were isolated from either *Foxp3*^{YFPcre} or Foxp3^{YFPcre} *Notch4*$^{/}$ mice that were sensitized with OVA and challenged with OVA+UFP. mRNA was isolated using Qiagen RNeasy mini kit (Qiagen). RNA was then converted into Double-stranded DNA (dsDNA), using SMART-Seq v4 Ultra Low Input RNA kit (Clontech). dsDNA was then fragmented to 200–300 bp size, using M220 Focused-ultrasonicator (Covaris), and utilized for construction of libraries for Illumina sequencing using KAPA Hyper Prep Kit (Kapa Biosystems). Libraries were then quantified using Qubit dsDNA HS (High Sensitivity) Assay Kit on Agilent High Sensitivity DNA Bioanalyzer.

Gene-level read counts were quantified using feature Counts and the latest UCSC mouse annotation (GRCm38/mm10). To identify differentially expressed genes, we used edgeR (version 3.28) and DESeq2 (version 1.26.0) Bioconductor packages with default parameters. Count tables were normalized to TPM (Transcripts per Million) for visualizations and QC. Sample clustering and path analyses were performed using a custom-made pipeline available upon request. Transcripts were called as differentially expressed when the adjusted p values were below 0.05, fold-changes over ±1.5 and false discovery rate (FDR) were below 0.1. Raw sequencing files will be accessible in the NCBI repository in the near future.

Statistical analysis.

Student's two-tailed t-test, one- and two-way ANOVA and repeat measures two-way ANOVA with Sidak post-test analysis of groups were used to compare test groups, as indicated. A p-value <0.05 was considered statistically significant.

Study approval.

Recruitment of human subjects was approved by the Institutional Review Board at Boston Children's Hospital and Marmara University. All animal studies were reviewed and approved by the Boston Children's Hospital office of Animal Care Resources.

Data Availability.

The data presented in the manuscript, including de-identified patient results, will be made available to investigators following request to the corresponding author. Any data and materials to be shared will be released via a material transfer agreement. RNA sequencing datasets have been deposited in the Gene Expression Omnibus with the accession code GSE151763.
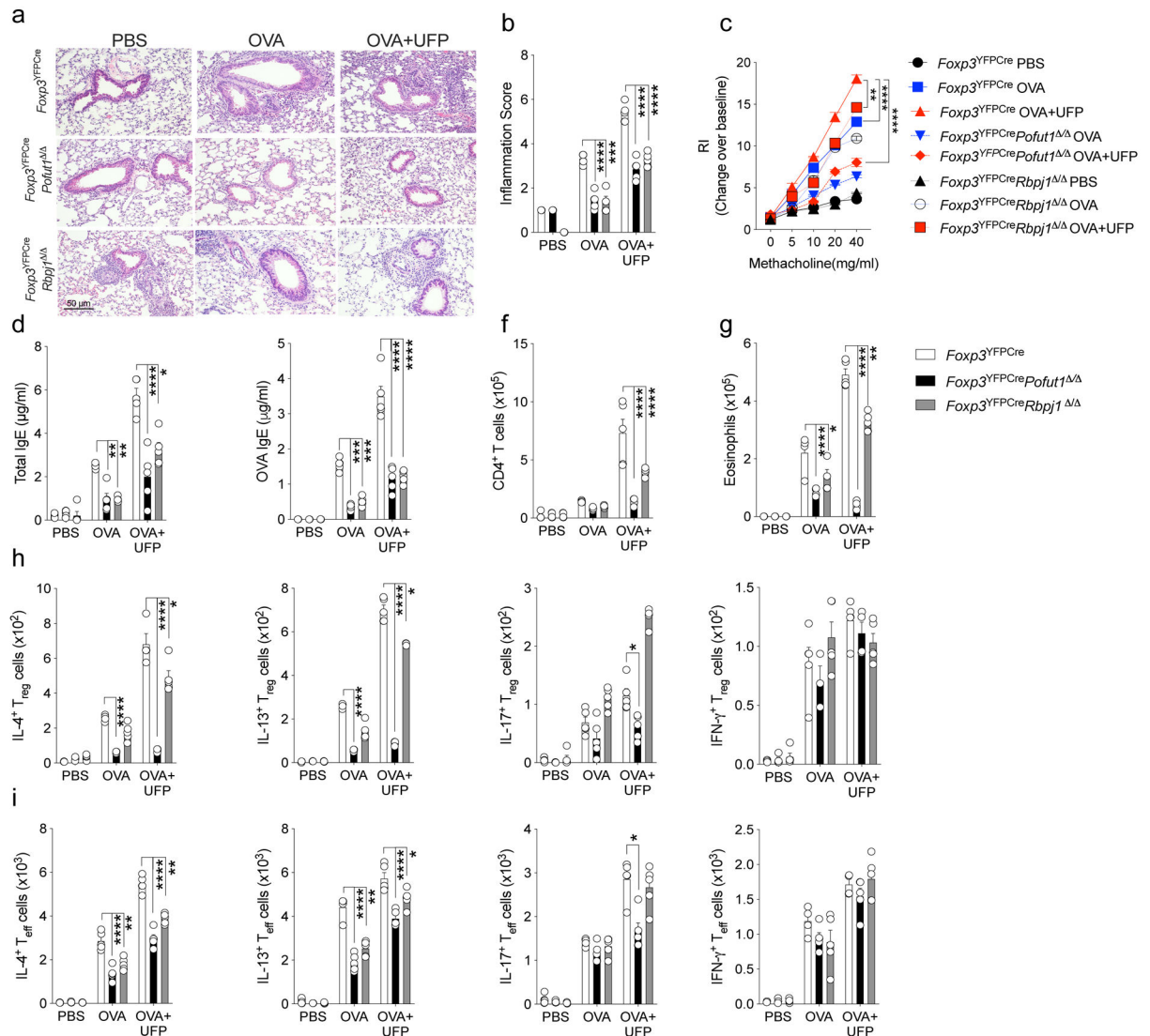
Extended Data
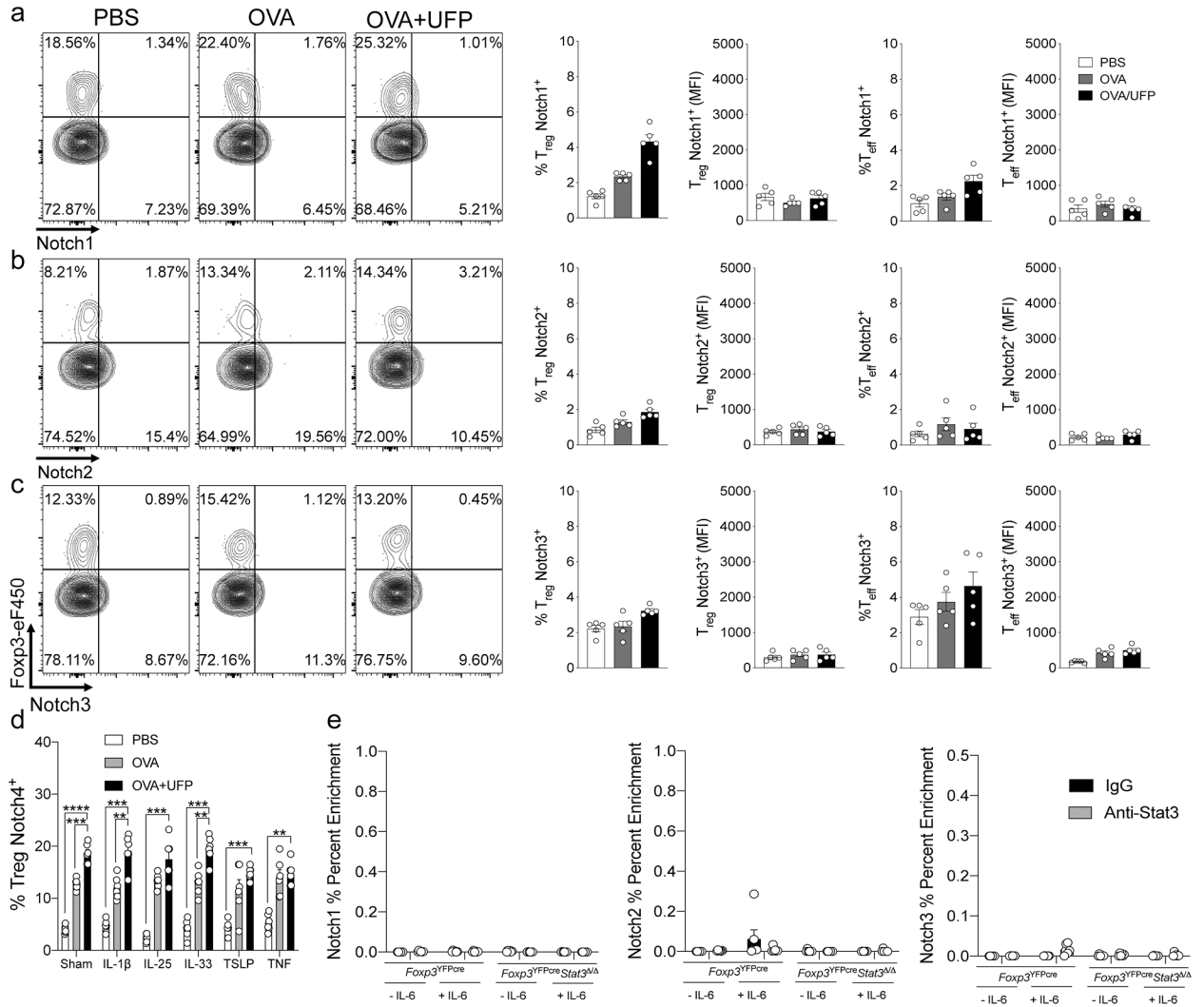
Extended Data Fig. 1. Notch4 expression on lung T_{reg} cells in allergic airway inflammation
a-c, Flow cytometric analysis, cell frequencies and (MFI) of Notch1, 2 and 3 expression on lung T_{reg} and T_{eff} cells in *Foxp3*[YFPCre] (n=5). **d**, Cell frequencies of Notch4 expression on OT-II^{+}CD4^{+}Foxp3^{+} T cells generated in co-cultures with sham or OVA[323–339]+UFP-pulsed alveolar macrophages without or with IL-1β, IL-25, IL-33, TSLP or TNF (n=5). **e**, ChIP assays for the binding of STAT3 and control (IgG) antibodies to the *Notch1, 2* and *3* promoters in lung T_{reg} cells of OVA+UFP-treated *Foxp3*[YFPCre], and *Foxp3*[YFPCre]*Stat3*[Δ/Δ]

mice (n=5). Each symbol represents one mouse. Numbers in flow plots indicate percentages. Error bars indicate SEM. Statistical tests: One-way ANOVA with Dunnett's post hoc analysis (**a-c**); two-way ANOVA with Sidak's post hoc analysis (**d,e**). **P<0.01, ***P<0.001, ****P<0.0001. Data representative of two or three independent experiments.
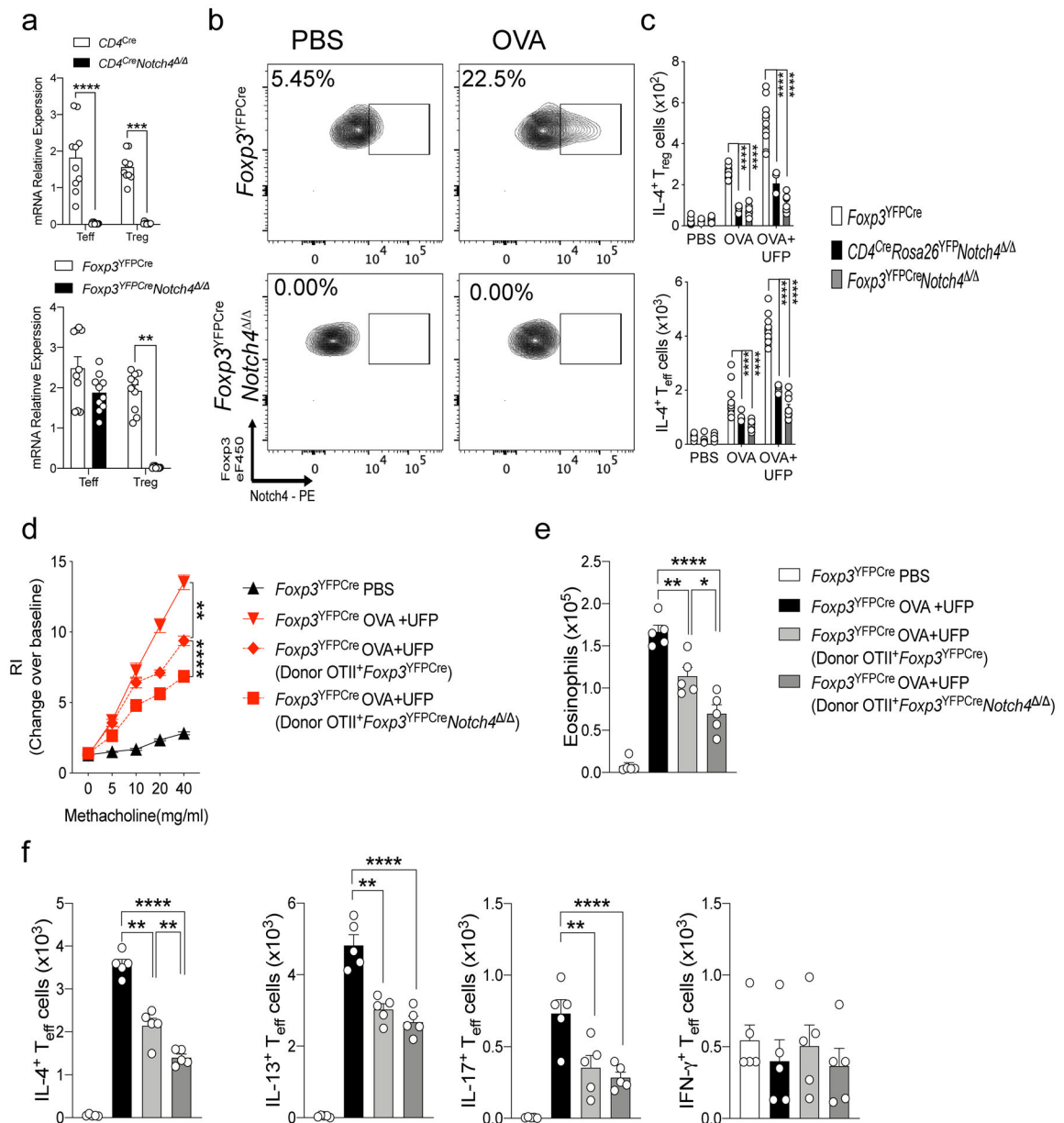
Extended Data Fig. 2. Notch4 expression on lung T_{reg} cells licenses allergic airway inflammation
a, RT-PCR analysis of Notch4 expression in $CD4^{Cre}$ mice in B-cells and T-cells (n=5). **b**, RT-PCR analysis of Notch4 expression in $Foxp3^{YFPCre}$ mice in both T_{reg} and T_{eff} cells (n=5). **c,d**, IL-4 and IFN-γ expression in lung Foxp3$^+$CD4$^+$ T_{reg}. (**c**) and Foxp3$^-$CD4$^+$T$_{eff}$ cells. (**d**) derived from the respectively treated $Foxp3^{YFPCre}$, $CD4^{Cre}Notch4^{/}$ and $Foxp3^{YFPCre}Notch4^{/}$ mice (n=5). **e**, Airway hyperresponsiveness in $Foxp3^{YFPCre}$

sensitized either with PBS or OVA, then challenged with OVA+UFP following transfer of OTII[+]$Foxp3$[YFPCre] or OTII[+]$Foxp3$[YFPCre]Notch4[/] iT$_{reg}$ cells (n=5). **f**, Eosinophil numbers for the respective mouse groups (n=5). **g**, IL-4, IL-13, IL-17 and IFNγ expression in lung Foxp3^{−}CD4^{−} T$_{eff}$ cells. Each symbol represents one mouse (n=5). Error bars indicate SEM. Statistical tests: two-way ANOVA with Sidak's post hoc analysis (**a,c,d**); One-way ANOVA with Dunnett's post hoc analysis (**e,f**). *P<0.05, **P<0.01, ***P<0.001, ****P<0.0001. Data representative of two or three independent experiments.
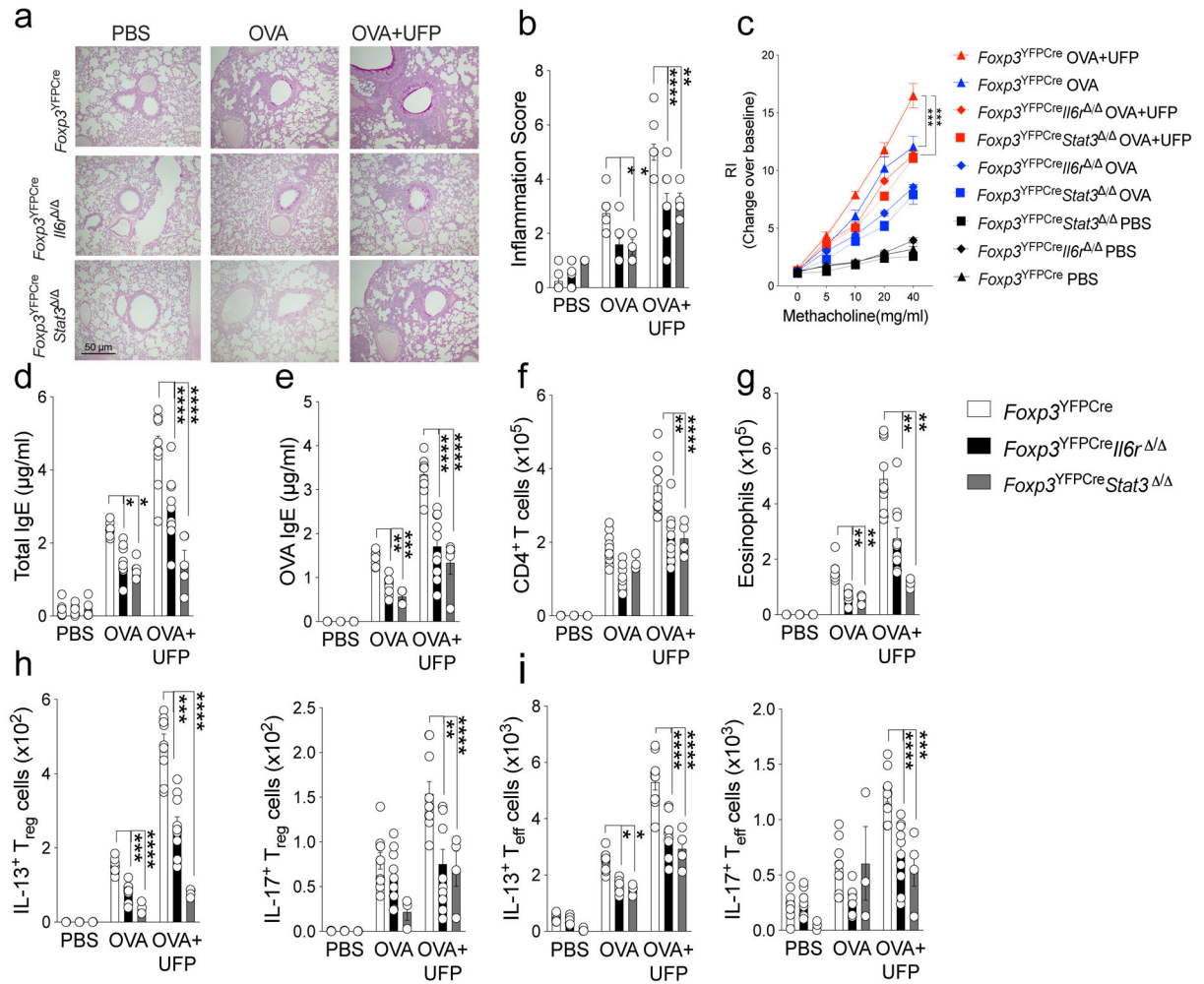

Extended Data Fig. 3. Allergic airway inflammatory responses in mice with T$_{reg}$ cell-specific *Pofut1* or *Rbpj1* deletion

a, Representative PAS-stained sections of lung tissues isolated from *Foxp3*[YFPCre], *Foxp3*[YFPCre]*Pofut1*[/] or *Foxp3*[YFPCre]*Rbpj1*[/] mice segregated into PBS, OVA or OVA +UFP-treated groups (200X magnification). **b**, Inflammation scores in the respective lung tissues. **c**, AHR in the respective mouse groups in response to methacholine. **d,e**, serum total and OVA-specific IgE concentrations. **f,g**, absolute numbers of lung CD4^{+} T cells and

eosinophils. **h,i,**IL-4, IL-13, IL-17 and IFNγ expression in lung $Foxp3^+CD4^+$ T_{reg} (**h**) and $Foxp3^-CD4^+T_{eff}$ cells (**i**). Each symbol represents an independent sample. Error bars indicate SEM. Statistical tests: two-way ANOVA with Sidak's post hoc analysis (**b-i**). *P<0.05, **P<0.01, ***P<0.001, ****P<0.0001. Data representative of two or three independent experiments. n=5 mice per group.
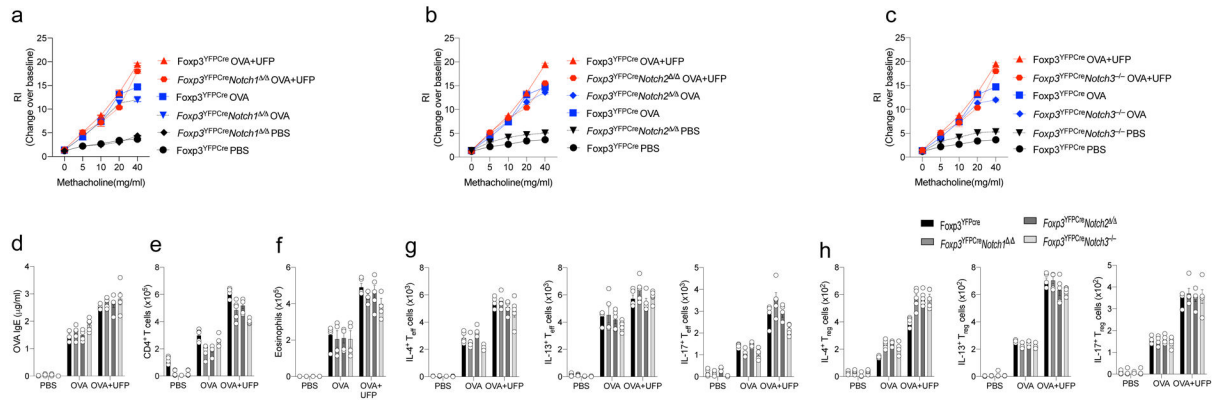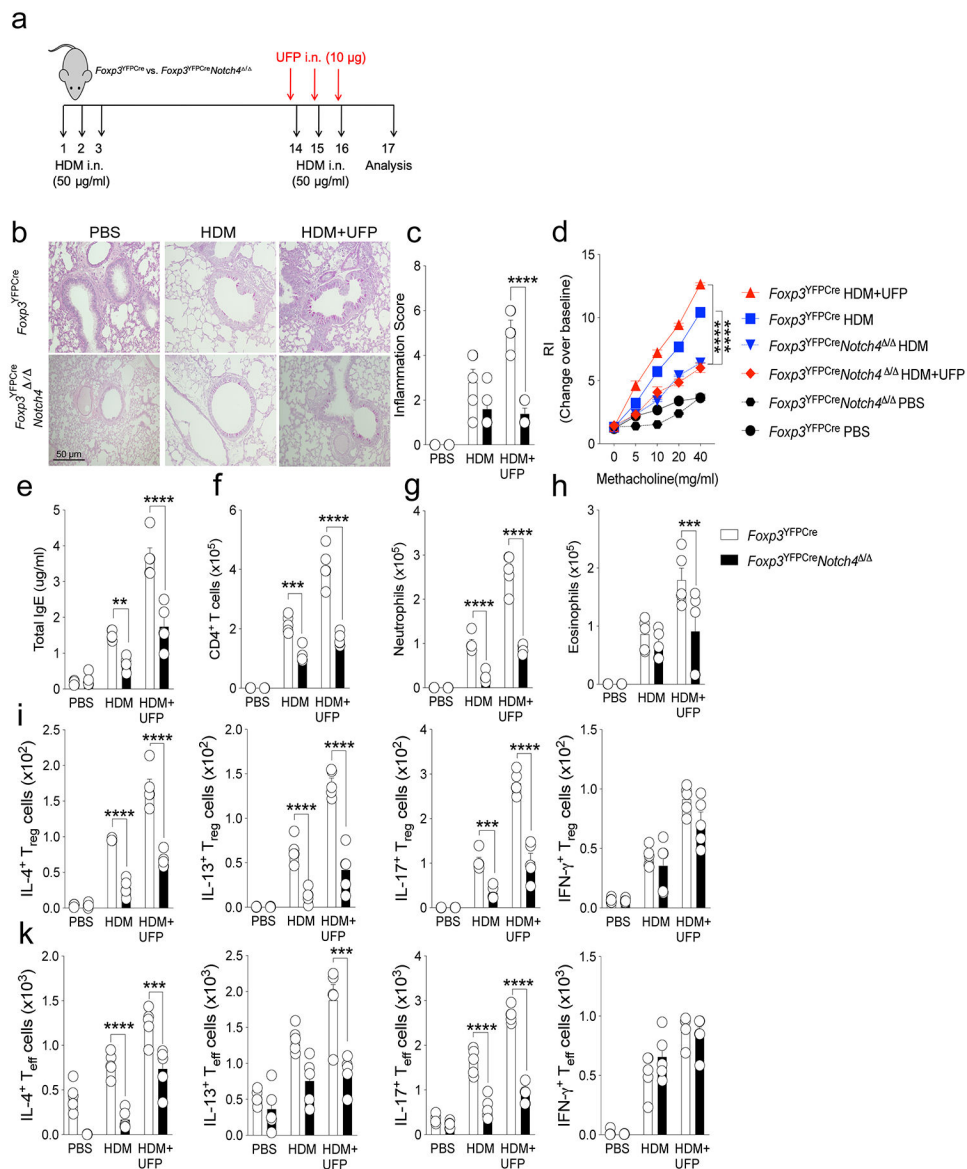

Extended Data Fig. 4. Allergic airway inflammatory responses in mice with T_{reg} cell-specific *Notch1 or Notch2* deletion or global *Notch3* deletion
a-**c**, AHR in *Foxp3*^{YFPCre}, *Foxp3*^{YFPCre}*Notch1*$^{/}$, *Foxp3*^{YFPCre}*Notch2*$^{/}$, or *Foxp3*^{YFPCre}*Notch3*$^{-/-}$ mice segregated into PBS, OVA or OVA+UFP-treated groups (200X magnification). **d**, serum OVA-specific IgE concentrations. **e,f**, absolute numbers of lung $CD4^+$ T cells and eosinophils. **g,h**, IL-4, IL-13, and IL-17 expression in lung $Foxp3^-$ $CD4^+T_{eff}$ (**g**) and $Foxp3^+CD4^+T_{reg}$ cells (**h**). Each symbol represents an independent sample. Error bars indicate SEM. Statistical tests: two-way ANOVA with Sidak's post hoc analysis **a-h**. Data representative of two or three independent experiments. n=5 mice per group.
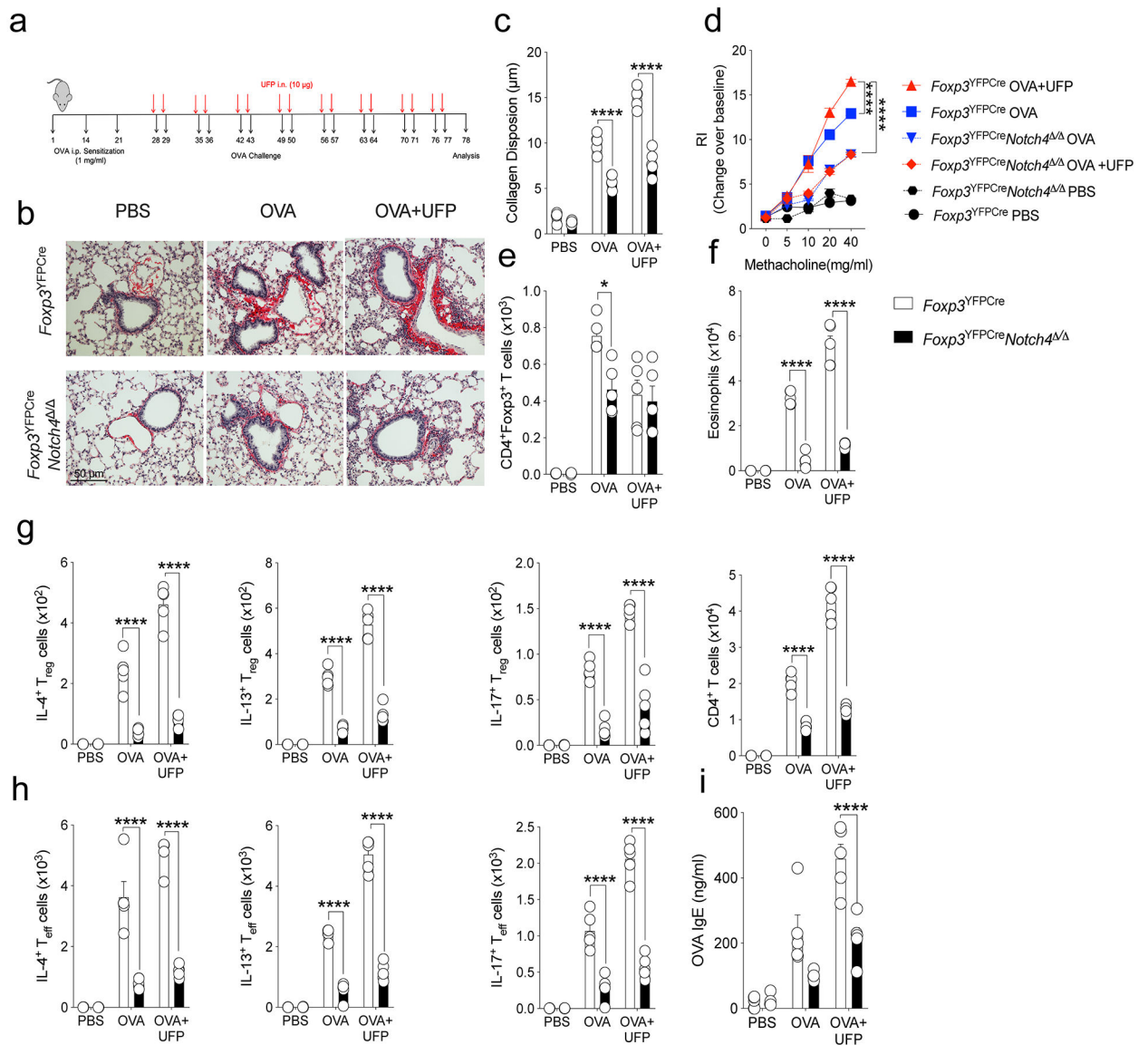
Extended Data Fig. 5. T_reg cell-specific *Il6r* and *stat3* deletions attenuate allergic airway inflammation

a, Representative PAS-stained sections of lung tissues isolated from *Foxp3*^{YFPCre}, *Foxp3*^{YFPCre}*Il6r*$^{/}$ or *Foxp3*^{YFPCre}*Stat3*$^{/}$ mice segregated into PBS, OVA or OVA+UFP-treated groups (200X magnification). **b**, Inflammation scores in the respective lung tissues. **c**, AHR in the respective mouse groups in response to methacholine. **d,e**, serum total and OVA-specific IgE concentrations. **f,g**, absolute numbers of lung CD4$^+$ T cells and eosinophils. **h,i**, IL-13 and IL-17 expression in lung Foxp3$^+$CD4$^+$ T_reg (**h**) and Foxp3$^-$CD4$^+$ T_eff cells (**i**). Each symbol represents an independent sample. Error bars indicate SEM. Statistical tests: two-way ANOVA with Sidak's post hoc analysis (**b-i**). *P<0.05, *P<0.05, **P<0.01, ***P<0.001, ****P<0.0001. Data representative of two or three independent experiments. n=5 mice per group.

Extended Data Fig. 6. T_reg cell-specific *Notch4* deletion rescues HDM induced allergic airway inflammation

a, scheme of the house dust mite (HDM) airway inflammation protocol. **b**, Representative PAS-stained sections of lung tissues isolated from *Foxp3*[YFPCre] or *Foxp3*[YFPCre]*Notch4*[/] mice segregated into PBS, OVA or OVA+UFP-treated groups (200X magnification). **c**, Inflammation scores in the respective lung tissues. **d**, AHR in the respective mouse groups in response to methacholine. **e**, serum total IgE concentrations. (**f-h**), absolute numbers of lung CD4^{+} T cells, neutrophils and eosinophils. **i,k**, IL-4, IL-13, IL-17 and IFNγ expression in lung Foxp3^{+}CD4^{+} T_reg (**i**) and Foxp3^{−}CD4^{+} T_eff cells (**k**). Each symbol represents an independent sample. Numbers in flow plots indicate percentages. Error bars indicate SEM. Statistical tests: two-way ANOVA with Sidak's post hoc analysis (**c-k**). **P<0.01, ***P<0.001, ****P<0.0001. Data representative of two or three independent experiments. n=5 mice per group.

Extended Data Fig. 7. T_reg cell-specific *Notch4* deletion rescues chronic allergic airway inflammation

a, Scheme for the chronic airway inflammation mouse protocol **b**, Representative Sirius-Red-stained sections of lung tissues isolated from *Foxp3*^YFPCre or *Foxp3*^YFPCre*Notch4* ^/^ mice segregated into PBS, OVA or OVA+UFP-treated groups (200X magnification). **c**, Collagen disposition measurement in the respective lung tissues. **d**, AHR in the respective mouse groups in response to methacholine. **e,f**, absolute numbers of lung CD4^+ T cells and eosinophils. **g,h**, IL-4, IL-13, and IL-17 expression in lung Foxp3^+CD4^+ T_reg (**g**) and Foxp3^–CD4^+T_eff cells (**h**). **i**, Serum OVA-specific IgE titers in the respective groups. Each symbol represents an independent sample. Error bars indicate SEM. Statistical tests: two-way ANOVA with Sidak's post hoc analysis (**c-h**). *P<0.05, ****P<0.0001. Data representative of two or three independent experiments. n=5 mice per group.
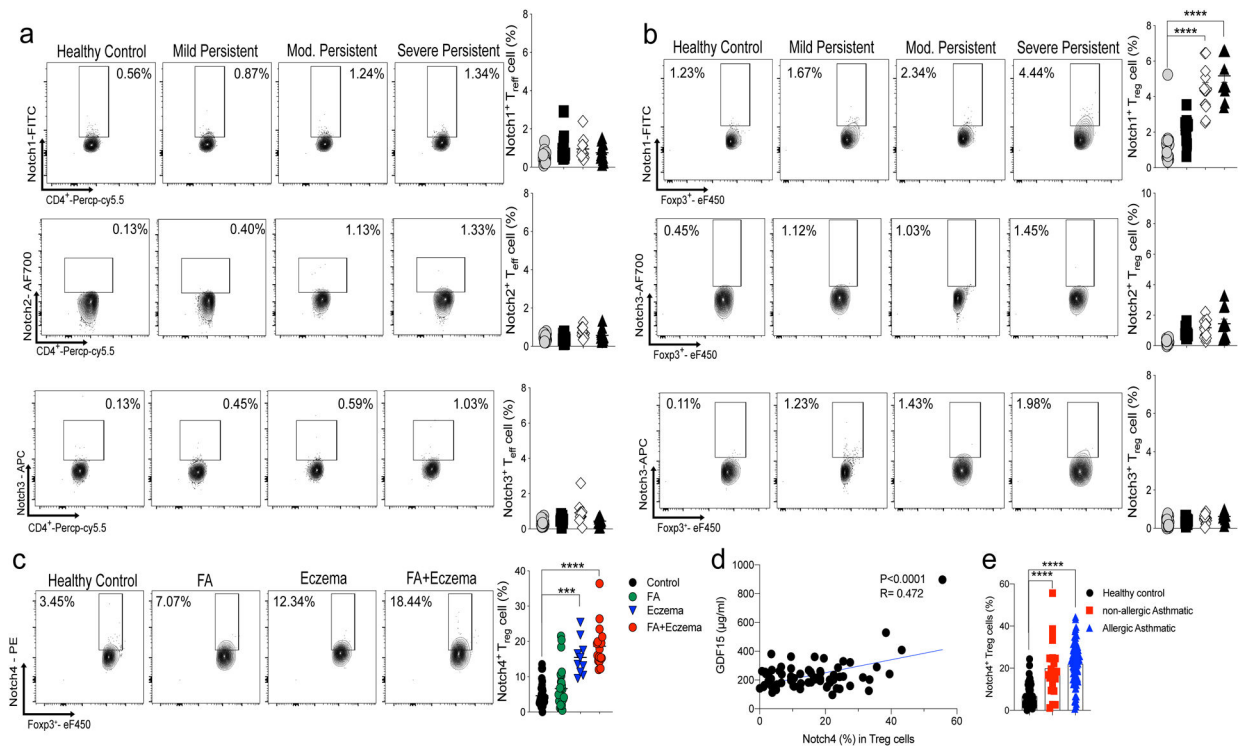
Extended Data Fig. 8. Notch receptor expression in human T_{reg} and T_{eff} cells

a,**b**, Flow cytometric analysis, cell frequencies and mean fluorescence intensity (MFI) of Notch1, 2 and 3 expression in peripheral blood T_{reg} cells (**a**) and T_{eff} cells (**b**) of control and asthmatic subjects, the latter segregated for asthma severity (control n=22, M.P n= 15, Mod n= 16. S.P n=11). **c**, Flow cytometric analysis and cell frequencies of Notch4 peripheral blood T_{reg} cells of healthy control, food allergy (FA), eczema and FA+eczema (Control n=37, FA n= 28, Eczema n=10 and FA+Eczema n=20) **d**, Serum GDF15 concentrations in asthmatic subjects plotted as a function of Notch4 expression on circulating T_{reg} cells (n=73) **e**, Cell frequencies of Notch4 expression in peripheral blood T_{reg} cells in healthy subjects, allergic and non-allergic asthmatics (control = 56, non-allergic n=21, allergic n=85). Error bars indicate SEM. Statistical tests: One-way ANOVA with Dunnett's post hoc analysis. (**a-c,e**); simple regression analysis (**d**). ***P<0.001, ****P<0.0001. Data representative of two or three independent experiments.

Supplementary Material

Refer to Web version on PubMed Central for supplementary material.

Acknowledgment

References

1. Lambrecht BN & Hammad H The immunology of asthma. Nat Immunol 16, 45–56 (2015). [PubMed: 25521684]

Nat Immunol. Author manuscript; available in PMC 2021 March 14.

2. Martinez FD & Vercelli D Asthma. Lancet 382, 1360–1372 (2013). [PubMed: 24041942]

3. Noval Rivas M & Chatila TA Regulatory T cells in allergic diseases. J Allergy Clin Immunol 138, 639–652 (2016). [PubMed: 27596705]

4. Krishnamoorthy N et al. Early infection with respiratory syncytial virus impairs regulatory T cell function and increases susceptibility to allergic asthma. Nat Med 18, 1525–1530 (2012). [PubMed: 22961107]

5. Noval Rivas M et al. Regulatory T cell reprogramming toward a Th2-cell-like lineage impairs oral tolerance and promotes food allergy. Immunity 42, 512–523 (2015). [PubMed: 25769611]

6. Massoud AH et al. An asthma-associated IL4R variant exacerbates airway inflammation by promoting conversion of regulatory T cells to TH17-like cells. Nat Med 22, 1013–1022 (2016). [PubMed: 27479084]

7. Xia M et al. Vehicular exhaust particles promote allergic airway inflammation through an aryl hydrocarbon receptor-notch signaling cascade. J Allergy Clin Immunol 136, 441–453 (2015). [PubMed: 25825216]

8. Xia M, Harb H, Saffari A, Sioutas C & Chatila TA A Jagged 1-Notch 4 molecular switch mediates airway inflammation induced by ultrafine particles. J Allergy Clin Immunol 142, 1243–1256 e1217 (2018). [PubMed: 29627423]

9. Tsai VWW, Husaini Y, Sainsbury A, Brown DA & Breit SN The MIC-1/GDF15-GFRAL Pathway in Energy Homeostasis: Implications for Obesity, Cachexia, and Other Associated Diseases. Cell Metab 28, 353–368 (2018). [PubMed: 30184485]

10. Luan HH et al. GDF15 Is an Inflammation-Induced Central Mediator of Tissue Tolerance. Cell 178, 1231–1244 e1211 (2019). [PubMed: 31402172]

11. Chen W et al. Conversion of peripheral CD4+CD25- naive T cells to CD4+CD25+ regulatory T cells by TGF-beta induction of transcription factor Foxp3. J Exp Med 198, 1875–1886 (2003). [PubMed: 14676299]

12. Shi S & Stanley P Protein O-fucosyltransferase 1 is an essential component of Notch signaling pathways. Proc Natl Acad Sci U S A 100, 5234–5239 (2003). [PubMed: 12697902]

13. Charbonnier LM, Wang S, Georgiev P, Sefik E & Chatila TA Control of peripheral tolerance by regulatory T cell-intrinsic Notch signaling. Nat Immunol 16, 1162–1173 (2015). [PubMed: 26437242]

14. Han H et al. Inducible gene knockout of transcription factor recombination signal binding protein-J reveals its essential role in T versus B lineage decision. Int Immunol 14, 637–645 (2002). [PubMed: 12039915]

15. Tachdjian R et al. Pathogenicity of a disease-associated human IL-4 receptor allele in experimental asthma. J Exp Med 206, 2191–2204 (2009). [PubMed: 19770271]

16. Shi H et al. Hippo Kinases Mst1 and Mst2 Sense and Amplify IL-2R-STAT5 Signaling in Regulatory T Cells to Establish Stable Regulatory Activity. Immunity 49, 899–914 e896 (2018). [PubMed: 30413360]

17. Geng J et al. The transcriptional coactivator TAZ regulates reciprocal differentiation of TH17 cells and Treg cells. Nat Immunol 18, 800–812 (2017). [PubMed: 28504697]

18. van Loosdregt J et al. Canonical Wnt signaling negatively modulates regulatory T cell function. Immunity 39, 298–310 (2013). [PubMed: 23954131]

19. van Loosdregt J & Coffer PJ The Role of WNT Signaling in Mature T Cells: T Cell Factor Is Coming Home. J Immunol 201, 2193–2200 (2018). [PubMed: 30301837]

20. Misra JR & Irvine KD The Hippo Signaling Network and Its Biological Functions. Annu Rev Genet 52, 65–87 (2018). [PubMed: 30183404]

21. Clevers H & Nusse R Wnt/beta-catenin signaling and disease. Cell 149, 1192–1205 (2012). [PubMed: 22682243]

22. Feng Y et al. Control of the inheritance of regulatory T cell identity by a cis element in the Foxp3 locus. Cell 158, 749–763 (2014). [PubMed: 25126783]

23. Li X, Liang Y, LeBlanc M, Benner C & Zheng Y Function of a Foxp3 cis-element in protecting regulatory T cell identity. Cell 158, 734–748 (2014). [PubMed: 25126782]

24. Vivier E et al. Innate Lymphoid Cells: 10 Years On. Cell 174, 1054–1066 (2018). [PubMed: 30142344]

25. Esty B et al. Treatment of severe persistent asthma with IL-6 receptor blockade. J Allergy Clin Immunol Pract 7, 1639–1642 e1634 (2019). [PubMed: 30885880]

26. Hirota T et al. Genome-wide association study identifies three new susceptibility loci for adult asthma in the Japanese population. Nat Genet 43, 893–896 (2011). [PubMed: 21804548]

27. Ferreira MA et al. Identification of IL6R and chromosome 11q13.5 as risk loci for asthma. Lancet 378, 1006–1014 (2011). [PubMed: 21907864]

28. Gruzieva O et al. Prenatal Particulate Air Pollution and DNA Methylation in Newborns: An Epigenome-Wide Meta-Analysis. Environ Health Perspect 127, 57012 (2019). [PubMed: 31148503]

29. Li X et al. Genome-wide association study identifies TH1 pathway genes associated with lung function in asthmatic patients. J Allergy Clin Immunol 132, 313–320 e315 (2013). [PubMed: 23541324]

30. Savenije OE et al. Association of IL33-IL-1 receptor-like 1 (IL1RL1) pathway polymorphisms with wheezing phenotypes and asthma in childhood. J Allergy Clin Immunol 134, 170–177 (2014). [PubMed: 24568840]

31. Soroosh P et al. Lung-resident tissue macrophages generate Foxp3+ regulatory T cells and promote airway tolerance. J Exp Med 210, 775–788 (2013). [PubMed: 23547101]

32. Magee CN et al. Notch-1 Inhibition Promotes Immune Regulation in Transplantation via Treg-Dependent Mechanisms. Circulation (2019).

33. Lee PP et al. A critical role for Dnmt1 and DNA methylation in T cell development, function, and survival. Immunity 15, 763–774 (2001). [PubMed: 11728338]

34. Messerschmidt D et al. beta-catenin-mediated adhesion is required for successful preimplantation mouse embryo development. Development 143, 1993–1999 (2016). [PubMed: 27246714]

35. Rubtsov YP et al. Regulatory T cell-derived interleukin-10 limits inflammation at environmental interfaces. Immunity 28, 546–558 (2008). [PubMed: 18387831]

36. McFarland-Mancini MM et al. Differences in wound healing in mice with deficiency of IL-6 versus IL-6 receptor. J Immunol 184, 7219–7228 (2010). [PubMed: 20483735]

37. Yang X et al. Notch activation induces apoptosis in neural progenitor cells through a p53-dependent pathway. Dev Biol 269, 81–94 (2004). [PubMed: 15081359]

38. McCright B, Lozier J & Gridley T Generation of new Notch2 mutant alleles. Genesis 44, 29–33 (2006). [PubMed: 16397869]

39. Krebs LT et al. Characterization of Notch3-deficient mice: normal embryonic development and absence of genetic interactions with a Notch1 mutation. Genesis 37, 139–143 (2003). [PubMed: 14595837]

40. Barnden MJ, Allison J, Heath WR & Carbone FR Defective TCR expression in transgenic mice constructed using cDNA-based alpha- and beta-chain genes under the control of heterologous regulatory elements. Immunol Cell Biol 76, 34–40 (1998). [PubMed: 9553774]

41. Moh A et al. Role of STAT3 in liver regeneration: survival, DNA synthesis, inflammatory reaction and liver mass recovery. Laboratory investigation; a journal of technical methods and pathology 87, 1018–1028 (2007). [PubMed: 17660847]

42. Zhang N et al. The Merlin/NF2 tumor suppressor functions through the YAP oncoprotein to regulate tissue homeostasis in mammals. Developmental cell 19, 27–38 (2010). [PubMed: 20643348]

43. Reginensi A et al. Yap- and Cdc42-dependent nephrogenesis and morphogenesis during mouse kidney development. PLoS Genet 9, e1003380 (2013). [PubMed: 23555292]

44. Binder AK et al. Expression of Human NSAID Activated Gene 1 in Mice Leads to Altered Mammary Gland Differentiation and Impaired Lactation. PLoS One 11, e0146518 (2016). [PubMed: 26745373]

45. Charbonnier LM et al. Functional Reprogramming of Regulatory T cells in the absence of Foxp3. Nat Immunol (in press) (2019).

46. Zheng Y et al. Role of conserved non-coding DNA elements in the Foxp3 gene in regulatory T-cell fate. Nature 463, 808–812 (2010). [PubMed: 20072126]

47. Povoleri GAM et al. Human retinoic acid-regulated CD161(+) regulatory T cells support wound repair in intestinal mucosa. Nat Immunol 19, 1403–1414 (2018). [PubMed: 30397350]
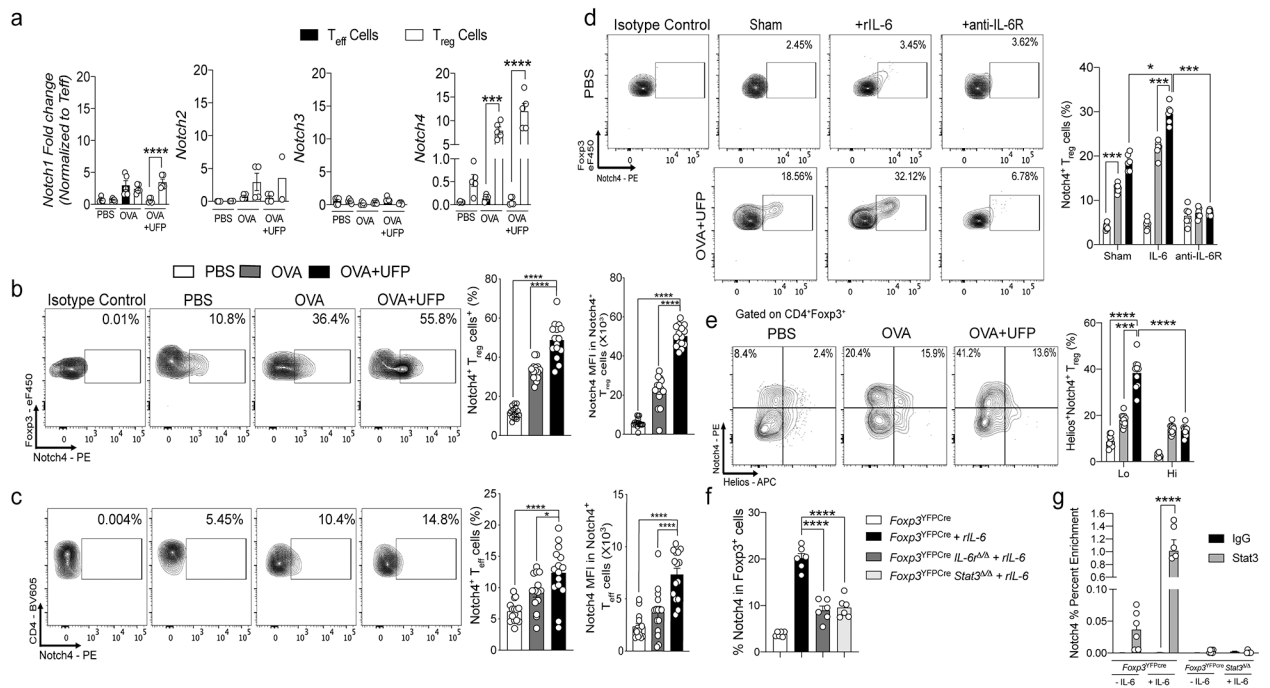
Fig. 1. Notch4 expression on lung T_reg cells in allergic airway inflammation.

a, RT-PCR of *Notch1-4* transcripts in lung T_reg and T_eff cells isolated from PBS, OVA and OVA+UFP mouse groups (n=5). **b,c**, Flow cytometric analysis, cell frequencies and mean fluorescence intensity (MFI) of Notch4 expression on lung T_reg and T_eff cells in the respective treated groups (n=15). **d**, Flow cytometric analysis and cell frequencies of Notch4 expression on OT-II$^+$CD4$^+$Foxp3$^+$ T cells generated in co-cultures with sham or OVA$_{323-339}$+UFP-pulsed alveolar macrophages without or with IL-6 or anti-IL-6R mAb (n=5). **e**, Flow cytometric analysis and cell frequencies of Notch4$^+$Helios$^-$ and Helios$^+$ lung T_reg cells isolated from the respective treated groups (n=5). **f**, Flow cytometric analysis and cell frequencies of Notch4 expression on *in vitro* differentiated T_reg cells derived from naive CD4$^+$ T cells isolated from *Foxp3*^{YFPCre}, *Foxp3*^{YFPCre}*Il6r*$^{/}$ and *Foxp3*^{YFPCre}*Stat3*$^{/}$ mice and either untreated or treated with IL-6 (n=6). **g**, ChIP assays for the binding of STAT3 and control (IgG) antibodies to the *Notch4* promoter in lung T_reg cells of OVA+UFP-treated *Foxp3*^{YFPCre}, and *Foxp3*^{YFPCre}*Stat3*$^{/}$ mice (n=6). Each symbol represents one mouse. Numbers in flow plots indicate percentages. Error bars indicate SEM. Statistical tests: One-way ANOVA with Dunnett's post hoc analysis (**b,c,f**); two-way ANOVA with Sidak's post hoc analysis (**a,d,e,g**). *P<0.05, ***P<0.001, ****P<0.0001. Data representative of two or three independent experiments.
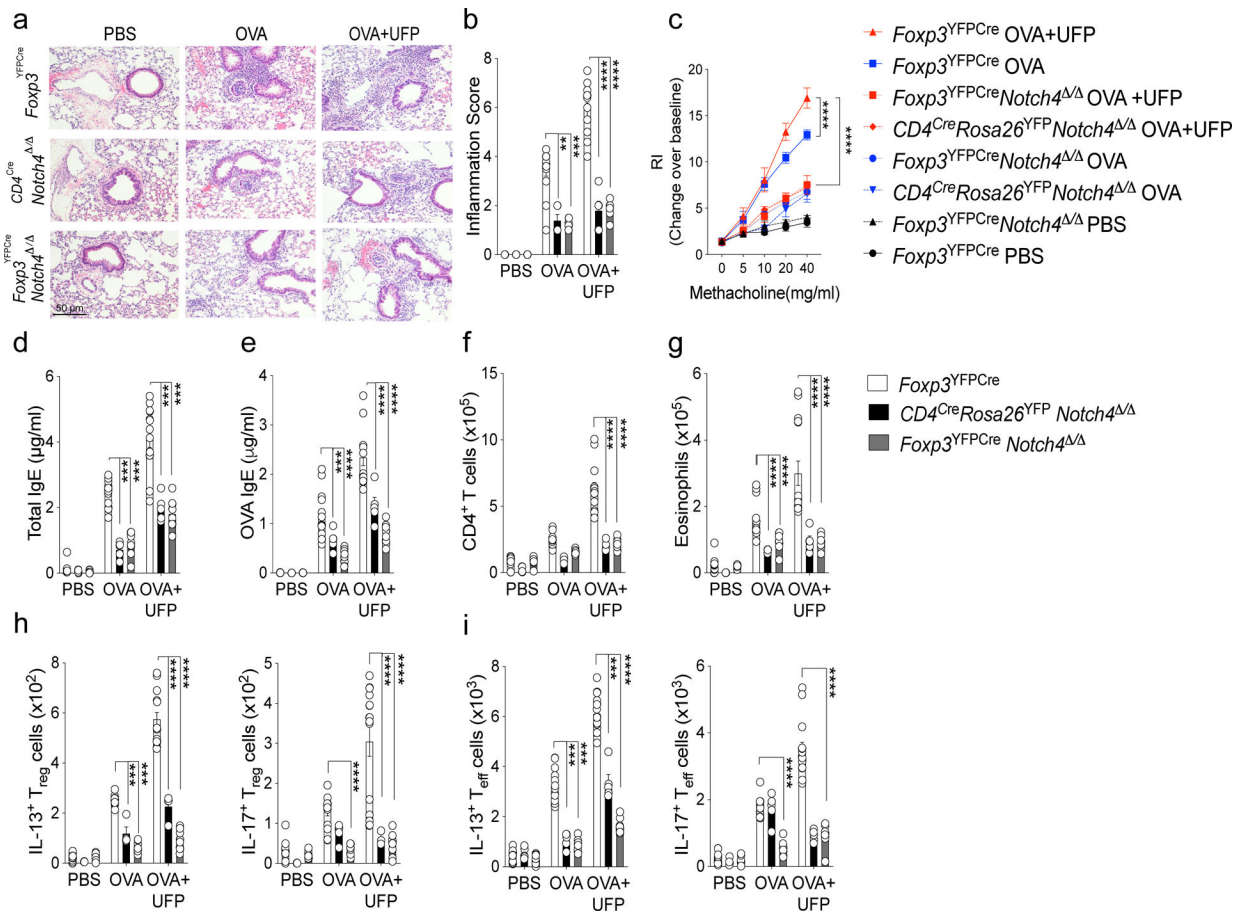
Fig. 2. Notch4 expression on lung T_reg cells licenses allergic airway inflammation.
a, Representative PAS-stained sections of lung tissues isolated from *Foxp3*^YFPCre,
CD4^Cre*Notch4*^/ or *Foxp3*^YFPCre*Notch4*^/ mice segregated into PBS, OVA or OVA+UFP-
treated groups (200X magnification). **b**, Inflammation scores in the respective lung tissues.
c, AHR in the respective mouse groups in response to methacholine. (**d,e**) serum total and
OVA-specific IgE concentrations. **f,g**, absolute numbers of lung CD4$^+$ T cells and
eosinophils. (**h,i**) IL-13 and IL-17 expression in lung Foxp3$^+$CD4$^+$ T_reg (**h**), and Foxp3$^-$
CD4$^+$ T_eff cells. (**i**). Each symbol represents an independent sample. Numbers in flow plots
indicate percentages. Error bars indicate SEM. Statistical tests: two-way ANOVA with
Sidak's post hoc analysis (**b-i**). **P<0.01, ***P<0.001, ****P<0.0001. Data representative
of two or three independent experiments. (White bars n=15), (black bars n=5) and (grey bars
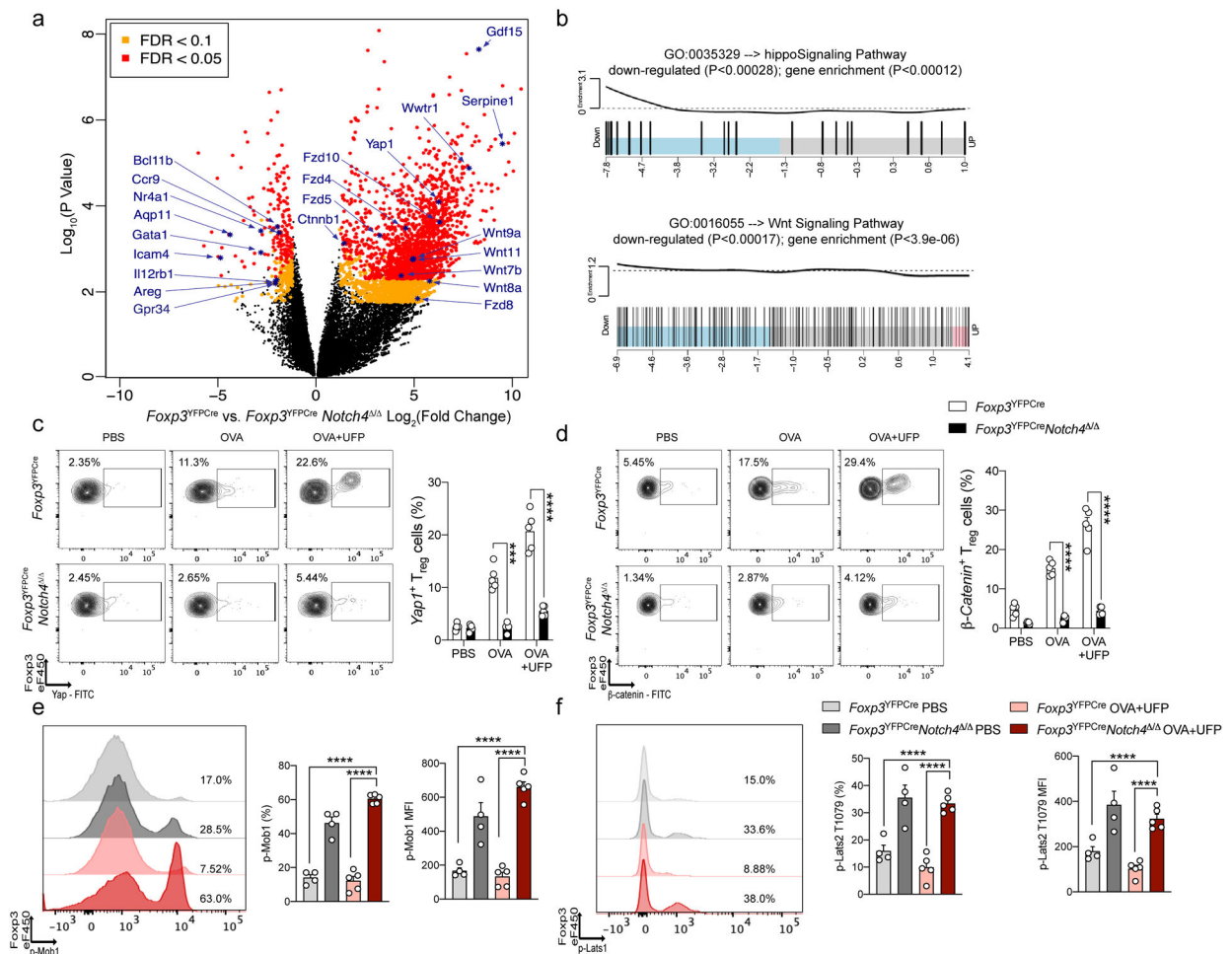n=15).

Fig. 3. Notch4-dependent transcriptional programs in lung T$_{reg}$ cells.
a, Volcano plot of differential gene expression in *Foxp3*^{YFPCre} versus *Foxp3*^{YFPCre}*Notch4*$^{/}$ T$_{reg}$ cells treated with OVA+UFP. FDR, false discovery rate; log2FC, log2(fold change). **b**, Enrichment pathway analysis of Hippo and Wnt pathways. **c,** Flow cytometric analysis and cell frequencies of Yap1 expression on lung T$_{reg}$ cells in the respective treated groups (n=5). **d,** Flow cytometric analysis and cell frequencies of β-Catenin expression on lung T$_{reg}$ cells in the respective treated groups (n=5). **e,** representative histogram, cell frequencies and MFI of phospho-Mob1 expression on lung T$_{reg}$ cells in the respective treated groups (light grey bar n= 4, dark grey bar n=4, light red bar n=5 and dark red bar n=4). **f,** representative histogram, cell frequencies and MFI of phospho-Lats1 T1079 expression on lung T$_{reg}$ cells in the respective treated groups (light grey bar n= 4, dark grey bar n=4, light red bar n=5 and dark red bar n=4). Each symbol represents an independent sample. Numbers in flow plots indicate percentages. Error bars indicate SEM. Statistical tests: two-way ANOVA with Sidak's post hoc analysis (**c,d**); one-way ANOVA with Dunnett's post hoc analysis (**e,f**). ***P<0.001, ****P<0.0001.
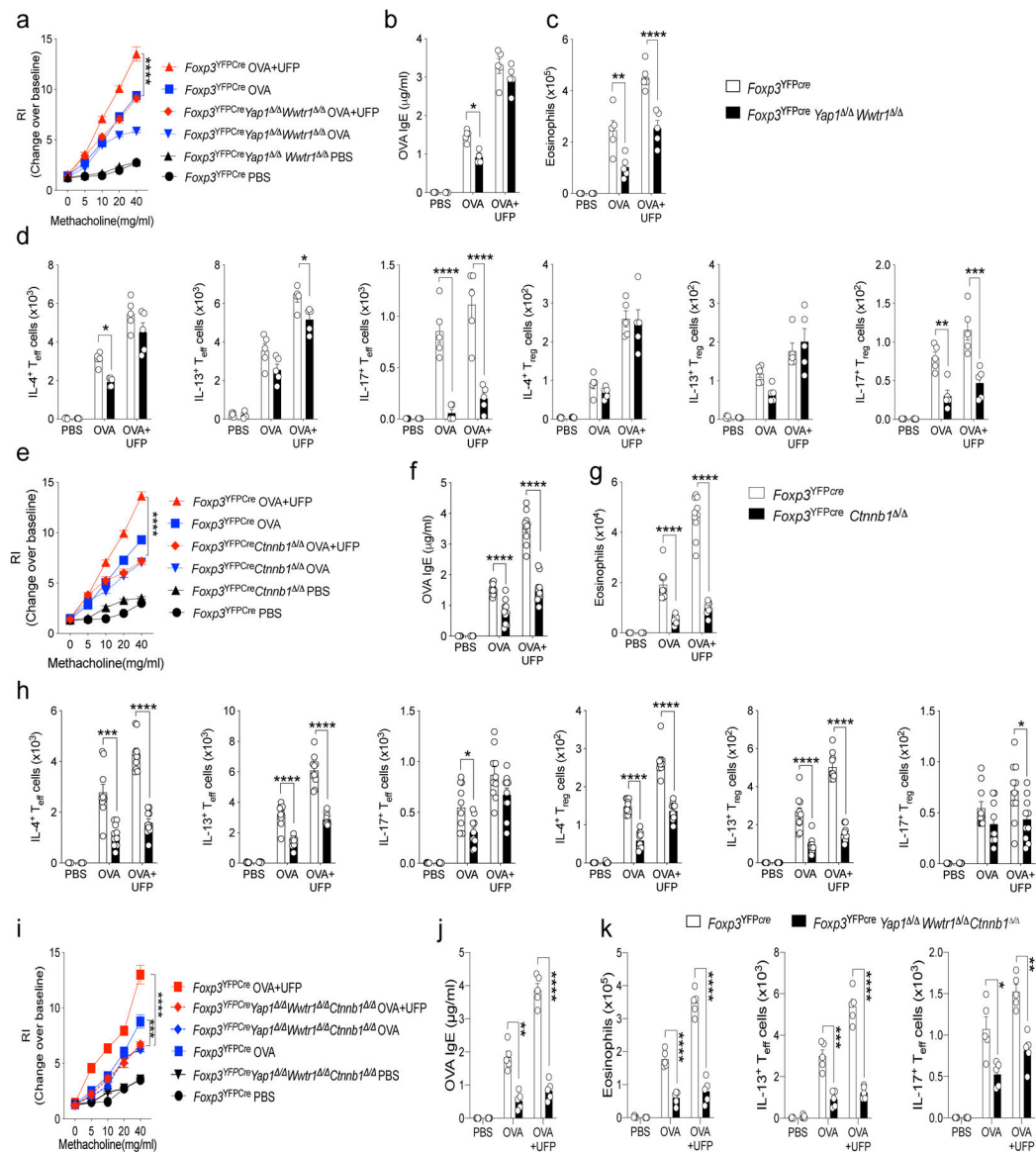
Fig. 4. Regulation of allergic airway inflammation by Notch4-dependent Hippo and Wnt pathway.

a,e,i, AHR in the respectively treated *Foxp3*[YFPCre] *Wwtr1*[/] *Yap1*[/] (**a**), *Foxp3*[YFPCre] *Ctnnb1*[/] mice (**e**) and *Foxp3*[YFPCre] *Wwtr1*[/] *Yap1*[/] *Ctnnb1*[/] (**i**) compared to control *Foxp3*[YFPCre] mice in response to methacholine (a, n=15, e, and i n=5). **b,f, and j** OVA specific IgE titers (b, n=15, f, and j n=5) (**c,d**, **g,h**, **k**) Absolute lung tissue eosinophils and IL-4+, IL-13+ and IL-17+ T_eff and T_reg cells in *Foxp3*[YFPCre] *Wwtr1*[/] *Yap1*[/] , *Foxp3*[YFPCre] *Ctnnb1*[/] and *Foxp3*[YFPCre] *Wwtr1*[/] *Yap1*[/] *Ctnnb1*[/] mice compared to control *Foxp3*[YFPCre] mice (c,d, n=15 g,h, k n=5). Each symbol represents an independent sample. Numbers in flow plots indicate percentages. Error bars indicate SEM. Statistical tests: two-way ANOVA with Sidak's post hoc analysis (**a-k**). *P<0.05, **P<0.01, ***P<0.001, ****P<0.0001. Data representative of two or three independent experiments.
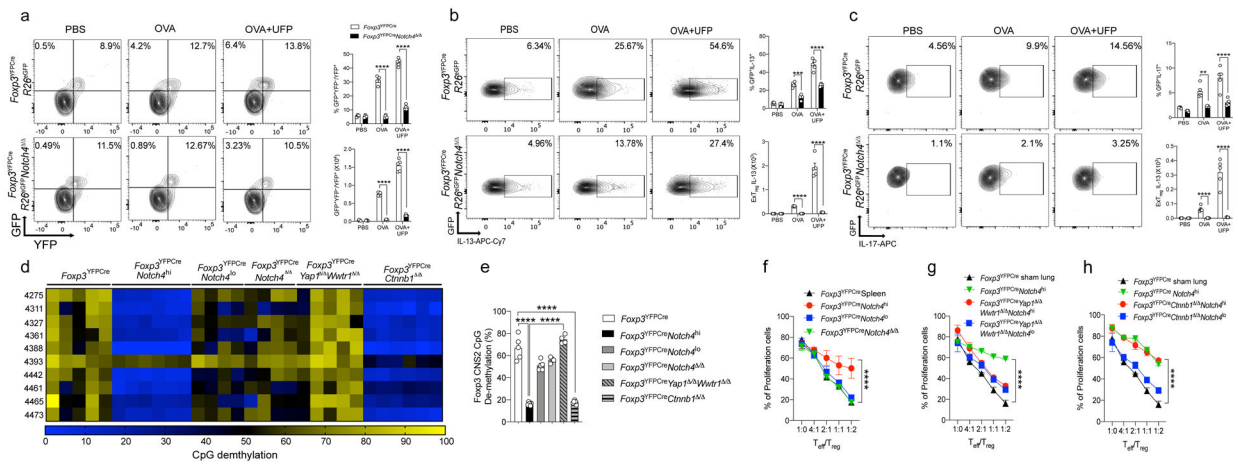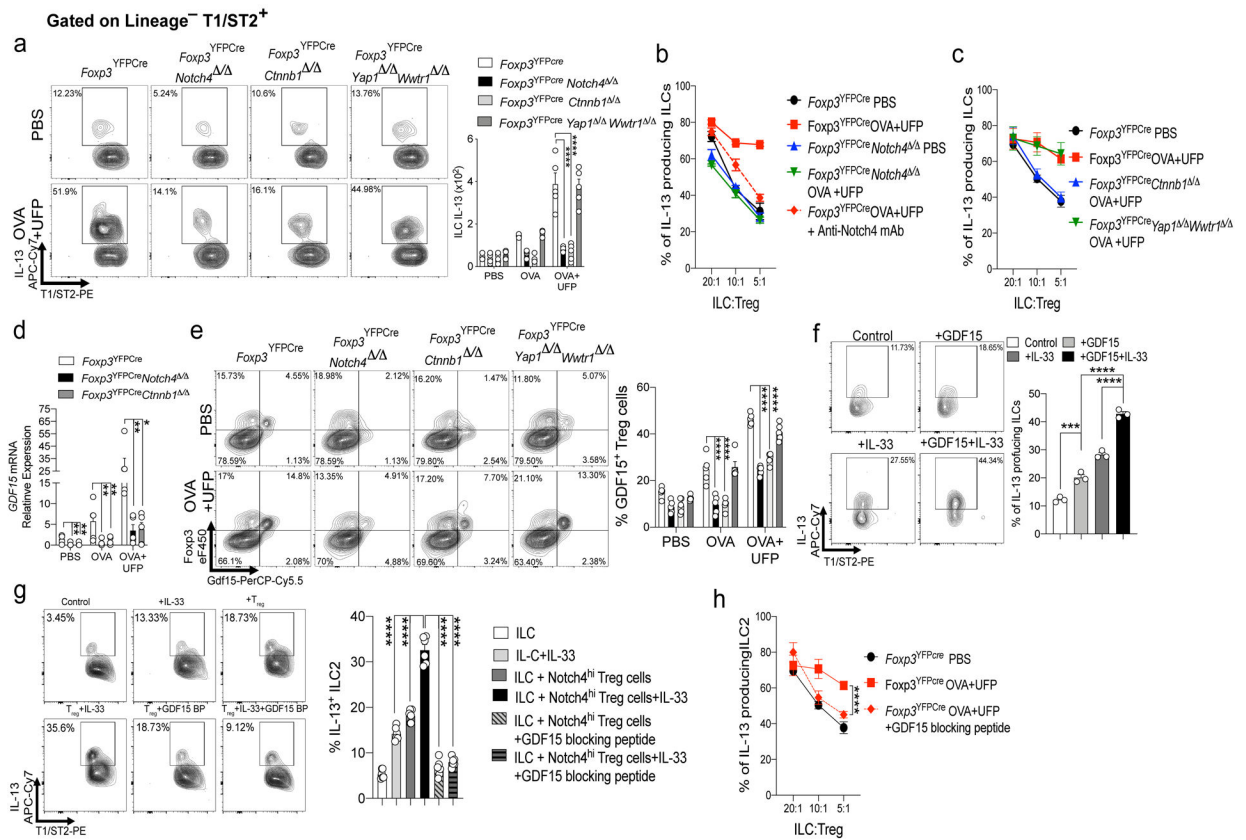
Fig. 5. Notch4 destabilizes T_reg cell in a Hippo pathway-dependent manner.
a, flow cytometric analysis and frequencies of exT_reg (GFP⁺YFP⁻) cells, plotted as a fraction of exT_reg to total T_reg (GFP⁺) cells in lung tissue (n=5). **b,c,** Flow cytometric analysis and frequencies of IL-13 (n=5) (**b**) and IL-17 (n=5) (**c**) producing exT_reg cells in lung tissues. **d**, Methylation status of CpG motifs of the foxp3 CNS2 region in T_reg cells isolated from lung tissue of sham versus OVA+UFP–sensitized and challenged mice of the respectively indicated genotypes. Numbers on the left side indicate the position of the respective motifs. **e**, Global methylation status of *Foxp3* CNS2 in the respective T_reg cell populations (white bar n=5, black bar n=6, dark grey bar n=5, light grey bar n=4, grey line bar n=4 and grey line bar n=6). **f**-**h**, *In vitro* suppression of the proliferation of WT responder CD4⁺ T cells (T_eff) by the respective T_reg cell populations (panel f, black line n=3, red line n=6, blue line n=6, green line n=3), (panel g, black line n=3 , green line n=3, red line n=3, blue line n=3) and (panel h, black line n=3, green line n=3, red line n=3, blue line n=3). Each symbol represents an independent sample. Numbers in flow plots indicate percentages. Error bars indicate SEM. Statistical tests: two-way ANOVA with Sidak's post hoc analysis (**a-c**) and (**f-h**); One-way ANOVA with Dunnett's post hoc analysis (**e**), **P<0.01, ****P<0.0001. Data representative of two or three independent experiments.
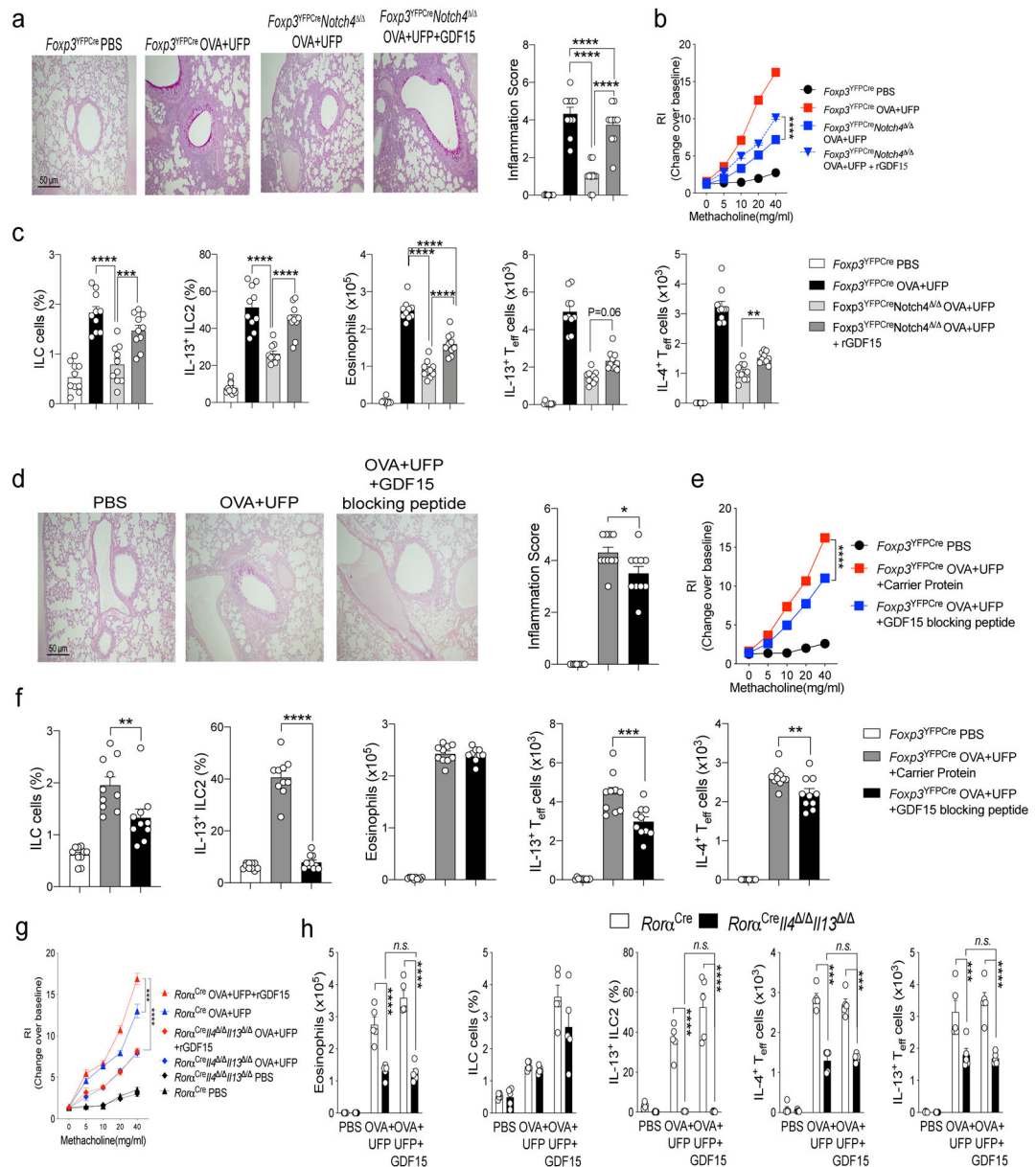
Fig. 6. Notch4 promotes ILC2 activation via a GDF15-dependent mechanism

a, flow cytometric analysis and frequencies of IL13+ ILC2 (Lineage−T1/ST2+ cells) in mice of respective genotypes treated as indicated (n=5). **b,c**, *In vitro* suppression assays using ILC2 from OVA+UFP-treated *Foxp3*^YFPCre^ mice and lung T_reg cells of the respective genotypes, treated as indicated (n=4) . **d**, GDF15 transcripts in T_reg cells of *Foxp3*^YFPCre^, *Foxp3*^YFPCre^*Notch4*^Δ/Δ^ and *Foxp3*^YFPCre^*Ctnnb1*^Δ/Δ^ (n=5). **e**, flow cytometric analysis and frequencies of GDF15+ lung T_reg cells in the respective mouse genotypes treated as indicated (n=5). **f**, flow cytometric analysis and frequencies of IL-13 induced in naive ILC2 stimulated with IL-33, GDF15 or both (n=3). **g**, IL-13 expression in naive ILC2 incubated with Notch4^hi^ T_reg cells from OVA+UFP treated mice without or with blocking GDF15 peptide (n=6). **h**, *In vitro* suppression assays using lung T_reg cells and ILC2 isolated from OVA+UFP-treated *Foxp3*^YFPCre^ mice and incubated without or with GDF15 blocking peptide (n=4). Each symbol represents an independent sample. Numbers in flow plots indicate percentages. Error bars indicate SEM. Statistical tests: two-way ANOVA with Sidak's post hoc analysis (**a-e,h**); One-way ANOVA with Dunnett's post hoc analysis (**f,g**). *P<0.05, **P<0.01, ***P<0.001, ****P<0.0001. Data representative of two or three independent experiments.

Fig. 7. GDF15 regulates ILC2 response in airway inflammation.

a,**d**, Representative PAS-stained sections of lung tissues isolated from *Foxp3*[YFPCre] and *Foxp3*[YFPCre]*Notch4*[Δ/Δ] with either PBS or OVA+UFP, the latter either alone or supplemented with GDF15 or GDF15 blocking peptide, as indicated (200X magnification), Inflammation score for the respective mouse groups (n=10). **b**,**e**, AHR in *Foxp3*[YFPCre] and *Foxp3*[YFPCre]*Notch4*[Δ/Δ] treated as indicated (n=10). **c, f**, Frequencies and absolute numbers of ILC2, eosinophils, IL-4, and IL-13, expression in lung Foxp3⁻CD4⁺ T_eff cells in the respective groups (n=10) **g,** AHR in *Rora*[Cre] and *Rora*[Cre]*Il4/Il13*[Δ/Δ] treated as indicated (n=5). **h,** Frequencies and absolute numbers of eosinophils, ILC2, IL-4, and IL-13, expression in lung Foxp3⁻CD4⁺ T_eff cells in the respective groups (n=5). Error bars indicate SEM. Statistical tests. One-way ANOVA with Dunnett's post hoc analysis. (**a,c,d,f**), two-

way ANOVA with Sidak's post hoc analysis (**b,e,g,h**); *P<0.05, **P<0.01, ***P<0.001, ****P<0.0001. Data representative of two or three independent experiments.
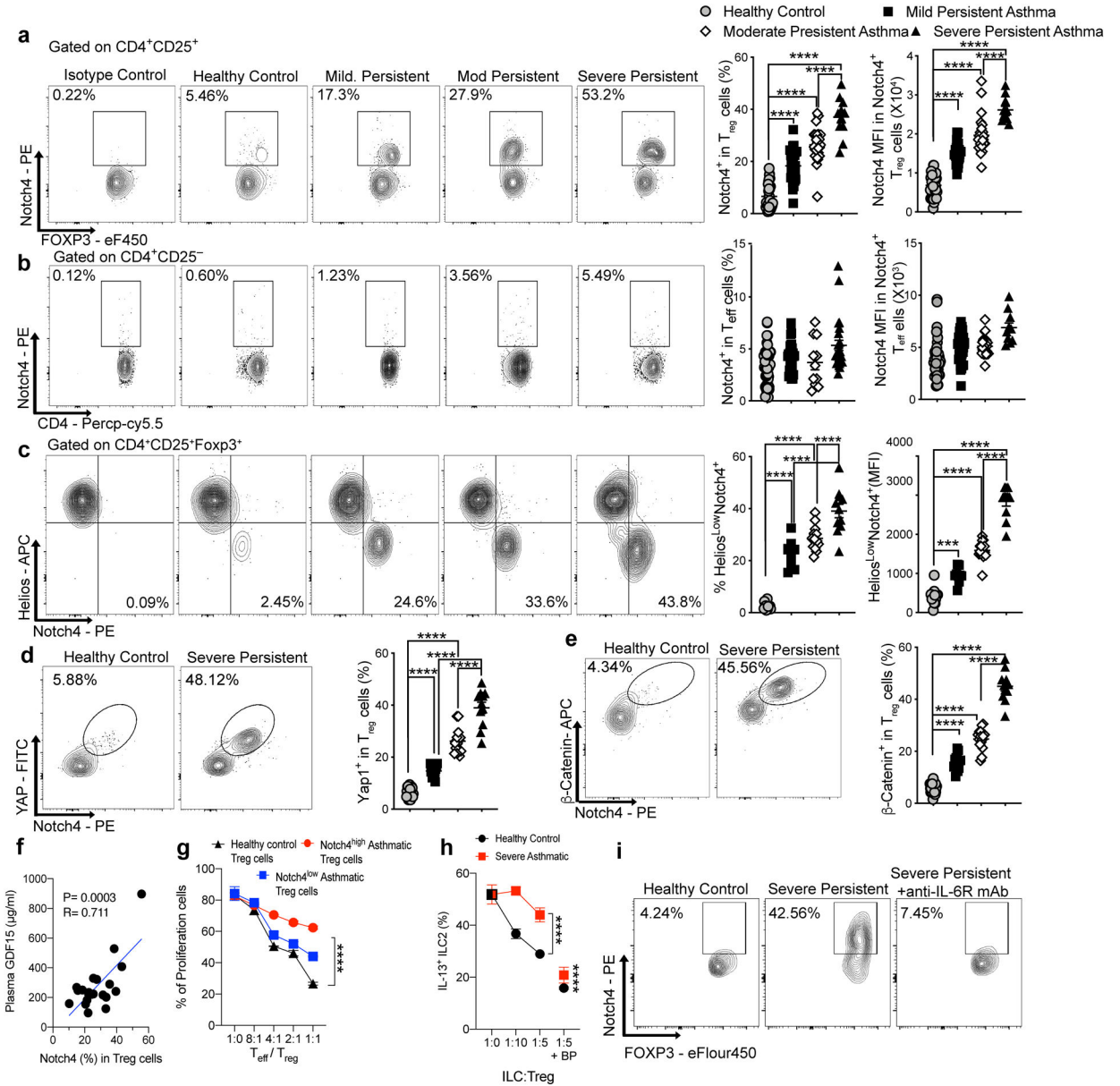
Fig. 8. Notch4 expression on circulating T_{reg} cells segregates with asthma severity.
a,**b**, Flow cytometric analysis, cell frequencies and MFI of Notch4 expression on circulating T_{reg} cells (**a**) and T_{eff} cells (**b**) of control and asthmatic subjects, the latter segregated for asthma severity (control: n=39; mild n=31; moderate: n=27; severe: n=11). **c**, flow cytometric analysis, cell frequencies and MFI of Notch4 expression on Helios$^+$ versus Helios$^-$ circulating T_{reg} cells of control and asthmatic subjects (control: n=13; mild n=9, moderate n=14; severe: n=11). **d**,**e**, Flow cytometric analysis, cell frequencies and MFI of Yap (**d**) and β-catenin (**e**) expression on circulating T_{reg} cells of control and severe asthmatic subjects (control n=24; mild n=15; moderate n=15; severe: n=11). **f**, Serum GDF15 concentrations in moderate and severe asthmatic subjects plotted as a function of Notch4 expression on circulating T_{reg} cells (n=21). **g**, *In vitro* suppression third party CD4$^+$ T cells (T_{eff}) by the Notch4^{hi} versus Notch4^{lo} T_{reg} cells from severe asthmatics compared to T_{reg}

cells of control subjects (n=2 subjects, 3 replicates per dilution per subject). **h,** *In vitro* suppression assays of ILC2 activation using circulating Notch4^{hi} T$_{reg}$ cells of asthmatics subjects and control T$_{reg}$ cells of healthy controls, incubated at the indicated T$_{reg}$ cell:ILC2 ratios without or with GDF15 blocking peptide (n=5). **i,** Flow cytometric analysis of Notch4 expression in T$_{reg}$ cells of a healthy control and a severe asthmatic before and after treatment with anti-IL-6R mAb (n=1). Error bars indicate SEM. Statistical tests: One-way ANOVA with Dunnett's post hoc analysis (**a-e**); simple linear regression analysis (**f**); two-way ANOVA with Sidak's post hoc analysis (**g,h**); ***P<0.001, ****P<0.0001. Data representative of two or three independent experiments.